THYMOQUINONE TRIGGERS DNA HYPOMETHYLATION IN HUMAN COLORECTAL ADENOCARCINOMA (CACO-2) CELLS

By

AALIYAH MANGERAH

222010501

BSc (Biochemistry and Physiology) (UNISA)

BMedSci Hons (Medical Biochemistry) (UKZN)

Supervisor: Prof. A. A. Chuturgoon

Co-supervisor: Dr. T. Ghazi

Submitted in fulfilment of the requirements for the degree of Master of Medical Science

In the Discipline of Medical Biochemistry

School of Laboratory Medicine and Medical Sciences, College of Health Sciences

University of KwaZulu-Natal, Durban, South Africa

2024

DECLARATION

I, Ms Aaliyah Mangerah, declare as follows:

i. The research reported in this thesis, except where otherwise indicated, is my original work.

ii. This thesis has not been submitted for any degree or examination at another university.

iii. This thesis does not contain other persons' data, pictures, graphs, or other information, unless specifically acknowledged as being sourced from other persons.

iv. This thesis does not contain other person's writing, unless specifically acknowledged as being sourced from other researchers. Where other written sources have been quoted, then:

a. their words have been re-written, but the general information sourced has been referenced to the authors.

b. where their exact words have been used, their writing has been placed within quotation marks and referenced.

v. Where I have reproduced a publication of which I am an author, co-author, or editor, I have indicated in detail which part of the publication was written by myself alone and have fully referenced such publications.

vi. This thesis does not contain text, graphics, or tables copied and pasted from the internet, unless specifically acknowledged, and the source is detailed in the thesis and reference section.

The research described in this study was carried out in the Discipline of Medical Biochemistry, School of Laboratory Medicine and Medical Sciences, College of Health Sciences, University of KwaZulu-Natal, under the supervision of Prof Anil A. Chuturgoon and Dr Terisha Ghazi.

Signed: 

Date: 06-12-2024

ACKNOWLEDGEMENTS

My husband, Yusuf

I couldn't have asked for a more supportive and understanding partner. Thank you for always encouraging me and being my biggest fan. You are everything to me.

My parents

My mother, **Rehana** – this literally would not have been possible without you. Thank you for driving me to Durban every week without complaining. You are the strongest woman I know, and I am so grateful for you. My father, **Faisal** – thank you for encouraging me through this venture, and for trying so hard to understand what my project was about. I truly appreciate all your love and support. My other set of parents, **Zaaheda** and **Ahmed** – your support and understanding means everything to me.

My supervisors, Dr Terisha Ghazi and Prof. Anil A. Chuturgoon

Dr Ghazi, I will forever be grateful for all your guidance and support. I will always cherish your patience and advice over these two years. Prof, thank you for accepting me into your research group and believing in me. I am thankful for both of you.

The Department of Medical Biochemistry

To the post-docs and senior lecturers – thank you for always being willing to lend a helping hand and showing up smiling. I appreciate you all. **Ms Ashmika Foolchand**, thank you for never hesitating to assist when I needed it, and providing lots of laughs. A special thank you to **Ms Zandile Ngwazi** – you were the best lab partner to laugh with and complain with. We finally made it!

My friends and family

Thank you for the endless support and encouragement. Yes, I've finally completed my Masters, you can stop asking me now.

My cats

My babies – **Basil**, **Luna**, **Missy**, **Joey**. Thank you for (sometimes) gracing me with cuddles and nose kisses. There's probably cat hair in this manuscript and I wouldn't have it any other way.

PRESENTATIONS

1. Thymoquinone triggers DNA hypomethylation in human colorectal adenocarcinoma (Caco-2) cells. A. Mangerah, T. Ghazi, A. A. Chuturgoon. School of Laboratory Medicine and Medical Sciences Research Day, University of KwaZulu-Natal, Durban, South Africa (27 September 2024). Oral Presentation.

CONTENTS

LIST OF ABBREVIATIONS

µL	Microlitre
µM	Micromolar
5-aza	5-azacytidine
5caC	5-carboxylcytosine
5fC	5-formylcytosine
5hmC	5-hydroxymethylcytosine
5mC	5-methylcytosine
AGO	Argonaute
ANOVA	Analysis of variance
APS	Ammonium persulfate
BCA	Bicinchoninic acid
BREC	Biomedical Research Ethics Committee
BSA	Bovine serum albumin
Caco-2	Colorectal adenocarcinoma cell line
cDNA	Complementary DNA
CH_3	Methyl group
CI	Confidence interval
CO_2	Carbon dioxide
CpG	Cytosine phosphate guanine
Cu^+	Cuprous ions
Cu^{2+}	Cupric ions
$CuSO_4$	Copper sulfate
DGCR8	DiGeorge syndrome critical region 8
dH_2O	Distilled water
DMEM	Dulbecco's modified eagle medium
DMSO	Dimethyl sulfoxide
DNA	Deoxyribonucleic acid
DNMT	DNA methyltransferase
EDTA	Ethylene diaminetetraacetic acid
ELISA	Enzyme-linked immunosorbent assay
FCS	Foetal calf serum

GAPDH	Glyceraldehyde-3-phosphate dehydrogenase
h	Hour
H_2O_2	Hydrogen peroxide
HAUSP	Herpesvirus-associated ubiquitin-specific protease
HCl	Hydrochloric acid
IC_{50}	Half-maximal inhibitory concentration
kg	Kilogram
LD_{50}	Lethal dose 50
MBD2	Methyl-binding-domain protein 2
mg	Milligram
min	Minute
miRNA	Micro-RNA
mL	Millilitre
mRNA	Messenger RNA
MTT	3-(4,5-dimethylthiazolyl-2)-2,5-diphenyltetrazolium bromide
ng	Nanogram
nm	Nanometre
NS	*Nigella sativa*
PBS	Phosphate buffered saline
PHD	Plant homeodomain
pre-miRNA	Precursor miRNA
pri-miRNA	Primary miRNA
qPCR	Quantitative polymerase chain reaction
RING	Really interesting new gene domain
RISC	RNA-induced silencing complex
RNA	Ribonucleic acid
RT	Room temperature
SAH	S-adenosyl homocysteine
SAM	S-adenosyl methionine
SD	Standard deviation
SDS	Sodium dodecyl sulphate
SDS-PAGE	Sodium dodecyl sulphate polyacrylamide gel electrophoresis
snoRNA	Small nucleolar RNA

SRA	Set and ring associated domain
TDG	Thymidine DNA glycosylase
TE	Tris-EDTA
TEMED	N, n, n', n' tetramethylethylenediamine
TET	Ten-eleven translocation
TQ	Thymoquinone
tRNA	Transfer RNA
TSG	Tumour suppressor gene
TTBS	Tris-buffered saline
TTD	Tandem tudor domain
UBL	Ubiquitin-like protein
UHRF1	Ubiquitin-like and RING finger domain 1
UTR	Untranslated region
V	Volts

LIST OF FIGURES

CHAPTER 2

CHAPTER 3

CHAPTER 4

CHAPTER 5

APPENDIX

LIST OF TABLES

ABSTRACT

DNA hypermethylation is a frequent feature of colorectal cancer, where it has been linked to the silencing of tumour suppressor genes and cancer progression. Thymoquinone (TQ) is a bioactive compound found in black cumin (*Nigella sativa*), and displays promising anti-cancer effects; however, its epigenetic effect in colorectal cancer is uncertain. This study investigated the impact of TQ on global DNA methylation in the human colorectal adenocarcinoma (Caco-2) cell line. Caco-2 cells were cultured and treated with TQ for 24 hours. The MTT assay was conducted to assess cell viability and obtain an IC_{50}. Global DNA methylation was quantified using an ELISA kit. Changes in mRNA expression of *DNMT1*, *DNMT3a*, *DNMT3b*, *UHRF1*, *MBD2*, *TET1*, *TET2*, *TET3*, and miR-29b were determined with qPCR. Changes in DNMT1, DNMT3a, DNMT3b, and MBD2 protein expression were assessed by Western blotting or ELISA. TQ dose-dependently decreased cell viability and yielded an IC_{50} of 504 μM. TQ brought about global DNA hypomethylation ($p < 0.005$) in Caco-2 cells. TQ reduced mRNA expression of *DNMT1* ($p < 0.05$), *DNMT3a* ($p < 0.05$), and *DNMT3b* ($p < 0.005$), as well as *UHRF1* ($p < 0.05$) and *MBD2* ($p < 0.05$). TQ increased *TET1* ($p < 0.05$), *TET2* ($p < 0.05$), and *TET3* mRNA expression ($p < 0.005$). MiR-29b expression was also increased ($p < 0.05$). TQ also reduced protein expression of DNMT1 ($p < 0.0001$), DNMT3a ($p < 0.0001$), DNMT3b ($p < 0.05$) and MBD2 ($p < 0.005$). Together, these results suggest that TQ induced global DNA hypomethylation in Caco-2 cells by down-regulating DNMT1, DNMT3a, DNMT3b, UHRF1, and MBD2, and up-regulating TET1-3 and miR-29b expression. This highlights the potential of TQ as a promising anti-cancer agent.

Keywords: thymoquinone, colorectal cancer, epigenetics, DNA methylation, microRNA

CHAPTER 1: INTRODUCTION

1.1. Background

Cancer is the second leading cause of death worldwide (Bray et al., 2021). Although having slightly decreased in recent years, the mortality rate is still staggeringly high (Global Burden of Disease Cancer et al., 2022). Based on statistics taken between 2018 and 2022, the mortality rate is reported to be 146 per 100 000 individuals (NCI, 2024). This statistic varies among sexes, with men showing a mortality rate of 173.2 per 100 000, and women 126.4 per 100 000 (NCI, 2024). The highest mortality rates are observed in older age groups of 50 years and above (CRUK, 2021). Notably, developing countries exhibit a cancer-related mortality rate of 66%: a figure that is disproportionately elevated (Grainger, 2023). This can be attributed to the high costs and limited availability of conventional treatment methods in the affected areas. Existing treatments are also known to cause a plethora of adverse effects. Chemotherapy and cancer drugs can result in debilitating fatigue, hair loss, a weakened immune system, blood clots, bruising and bleeding, memory fog, eyesight changes, nerve changes, infertility, liver and kidney problems, among others (CRUK, 2023, NHS, 2025). Immunotherapy can bring about skin reactions, flu symptoms, heart palpitations, inflammation, hyper- or hypotension, and dizziness (NCI, 2023). Even targeted therapies have adverse effects such as mouth sores, abnormal blood clotting, liver problems, and hypertension (NCI, 2022). Therefore, it remains necessary to explore alternative treatments that circumvent these issues.

Colorectal adenocarcinoma is described as a malignancy of colorectal tissue, and is the second most deadly type of cancer: 1.1 million annual deaths from colorectal cancer are projected to occur by the year 2030 (Rawla et al., 2019). The issues mentioned above are applicable to this type of cancer as well, making it imperative to focus research in this area to decrease the mortality rate. Natural compound-based therapeutics may prove to be a promising approach, given their high availability, affordability, and accessibility. In fact, several existing anticancer drugs (Taxol, epothilones) were formulated from natural product origins (Kim and Kim, 2018).

The term ‘epigenetics’ was first created in the 1940s by the biologist C. H. Waddington (Waddington, 2012) and refers to altered gene expression without changes in gene sequences (Holliday, 2006). The most common types of epigenetic changes are DNA methylation, histone modifications, and non-coding RNAs (Baylin and Ohm, 2006). These play regulatory functions in gene expression: DNA methylation results in transcriptional silencing, histone modifications

can either activate or silence gene expression, and microRNAs inhibit gene expression at the post-transcriptional level (Casey, 2016). Disruptions in these modifications cause abnormal gene expression, which contributes to various diseases, including cancer (Casey, 2016).

DNA methylation entails the incorporation of a CH_3 (methyl) group onto the fifth carbon of cytosine on promoter CpG islands to produce 5-methylcytosine (5mC) (Moore et al., 2013). This facilitates transcriptional silencing by inhibiting transcription factor binding to gene promoter regions (Razin and Kantor, 2005). DNA methyltransferases (DNMTs) are responsible for this phenomenon. Demethylation occurs by means of ten-eleven translocation (TET) proteins: 5mC is converted back to cytosine through a series of reactions (Wu and Zhang, 2017).

MicroRNAs (miRNAs) function by post-transcriptionally repressing gene expression through the targeting of specific mRNA for degradation (Bushati and Cohen, 2007). MiR-29b is of particular interest here, since it is reported to regulate the expression of DNMT proteins and therefore, influences DNA methylation (Kwon et al., 2019).

DNA hypermethylation is observed in almost all cancers, including colorectal cancer, with decreased expression of tumour suppressor genes to facilitate uncontrolled tumour cell proliferation (Nishiyama and Nakanishi, 2021). The expression of DNMT proteins is reportedly elevated, along with their associated cofactors (Liao et al., 2019). Conversely, TET proteins and miR-29b are downregulated (Kohli and Zhang, 2013, Jiang et al., 2014). Epigenetic changes are reversible, making them a promising target for drug development (Zhang et al., 2020a). Treatments that target these modifications may restore normal gene expression and reduce tumour cell survival and proliferation.

Thymoquinone (TQ) is found primarily in the herb *Nigella sativa* (NS), which has been used in the Middle East and Northern Africa for culinary and medicinal purposes for hundreds of years (Hannan et al., 2021). Historically, NS has been given great importance for its mentions in Islamic and Christian texts (Dalli et al., 2021), and it has been proven to possess a vast array of healing properties. The major bioactive compound in NS is TQ, which has demonstrated numerous therapeutic properties against conditions such as cancer, diabetes, hypertension, cardiovascular disease, inflammation, and neuropathies (Hannan et al., 2021). Its anticancer effects are the most widely studied, and it has proven to affect aberrant epigenetic machinery in several types of cancers (Khan et al., 2019). However, its effects on the epigenetic machinery in colorectal cancer remain unclear.

1.2. Aim, hypothesis, and objectives

Aim

This study aimed to determine the impact of TQ on the global DNA methylation status of Caco-2 cells.

Hypothesis

It was hypothesised that TQ induces global DNA hypomethylation in Caco-2 cells.

Null hypothesis

TQ has no significant effect on the global DNA methylation status of Caco-2 cells.

Objectives

The effects of TQ on Caco-2 cells were determined by measuring:

1) Cell viability using the MTT assay
2) Global DNA methylation using a DNA methylation quantification ELISA kit
3) DNA methylation/demethylation regulators using:
   - Western blot analysis of DNMT1, DNMT3a, and MBD2
   - ELISA analysis of DNMT3b
   - qPCR analysis of *DNMT1*, *DNMT3a*, *DNMT3b, UHRF1, MBD2*, *TET1*, *TET2*, *TET3*, and miR-29b expression

1.3. Research questions

1) Will TQ be toxic to Caco-2 colorectal adenocarcinoma cells?
2) Will TQ influence global DNA methylation in Caco-2 cells?
3) Will TQ affect the expression of DNMTs, the cofactor UHRF1, the methylation reader MBD2, and miR-29b?
4) If global DNA hypomethylation is observed, will TQ affect the expression of the demethylase TET1-3 proteins?

CHAPTER 2: LITERATURE REVIEW

2.1. Cancer

Cancer remains to be a global health burden that is predicted to plague humanity for decades (Foreman et al., 2018). A staggering 23.6 million new cancer cases were diagnosed globally in 2019, with 10 million deaths (Global Burden of Disease Cancer et al., 2022). The mortality rate associated with cancer is disproportionally higher in developing countries; this can be attributed to the high costs and inaccessibility of conventional treatment methods (Grainger, 2023). Given this, it is necessary to consider alternative treatment options that circumvent existing barriers, and natural compounds such as thymoquinone (TQ) may prove to be a promising option.

2.1.1. Cancer biology

A tumour is explained as a group or colony of cells that exhibit uncontrolled proliferation and can metastasise and invade tissues other than the tissue of origin (Roy and Saikia, 2016). The general cause can be attributed to defective regulation of the cell cycle, which ultimately results in 'immortal' cells that resist cell death signals (Vaghari-Tabari et al., 2021).

The genes involved in tumorigenesis can be divided into two broad categories – oncogenes and tumour suppressor genes (TSGs) (Figure 2.1). Oncogenes, derived from mutated proto-oncogenes, encode proteins that stimulate cell proliferation and ensure cell survival (Vaghari-Tabari et al., 2021). They stimulate tumorigenesis and, as can be expected, are overexpressed in cancers (Soleimani et al., 2019). Examples of oncogenes are Ras, Raf, ERK, Myc, and anti-apoptotic proteins (Luke et al., 2014). Conversely, tumour suppressor genes encode proteins that ensure cell cycle regulation, DNA damage repair, and apoptosis (Vaghari-Tabari). They inhibit tumorigenesis and are under-expressed in cancers. Notable examples are p53, p21, p27, and pro-apoptotic proteins (Liang et al., 2002, Ogawara et al., 2002).

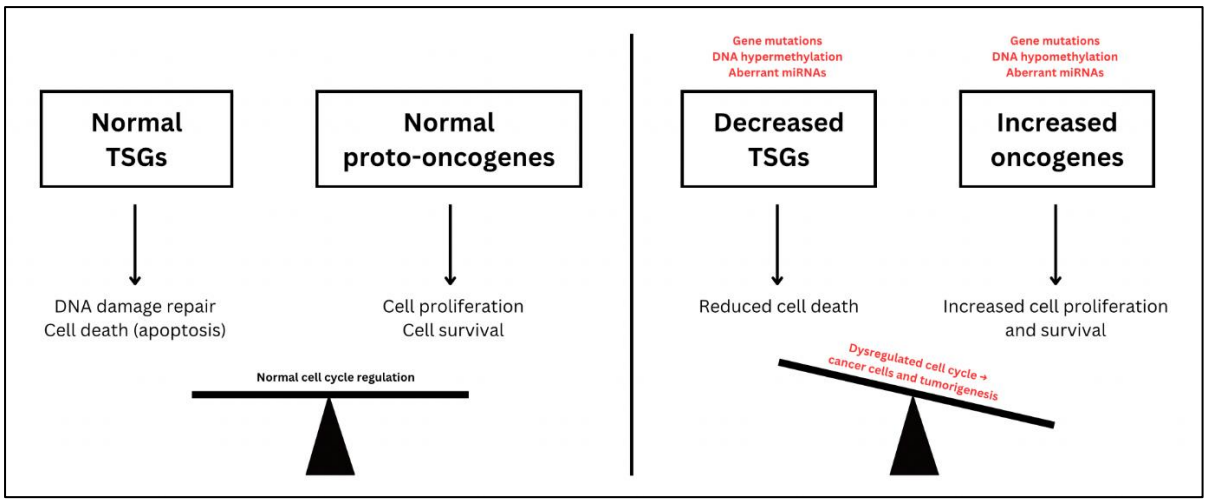

Figure 2.1: The role of oncogenes and tumour suppressor genes in the development and progression of cancer. TSGs: tumour suppressor genes (prepared by author).

Over- and under-expression of oncogenes and TSGs occur largely through the action of carcinogens, which are broadly categorised into genotoxic and epigenetic types. Genotoxic carcinogens cause gene mutations that result in increased oncogene expression and/or decreased TSG expression, ultimately causing uncontrolled growth of tumour cells (Diori Karidio and Sanlier, 2021). Epigenetic carcinogens also alter gene expression to cause uncontrolled tumour cell growth; however, they do so without changing the genetic sequences of oncogenes and TSGs (Diori Karidio and Sanlier, 2021). Rather, they affect gene expression through epigenetic alterations such as DNA methylation and microRNA aberrations, and their roles in cancer are explained in further detail in later sections.

2.1.2. Colorectal cancer

According to the World Health Organisation, colorectal cancer ranks as the third most frequently diagnosed cancer, with 1.8 million new diagnoses reported annually (WHO, 2023). It is reportedly the second most deadly cancer across the globe, with an approximate annual occurrence of 900 000 deaths (WHO, 2023). Colorectal cancer has shown an increased incidence of diagnosis in developing countries in recent years (WHO, 2023). Alarmingly, fewer than 20% of individuals diagnosed with metastatic colorectal cancer survive beyond five years from being diagnosed (Biller and Schrag, 2021).

As is evident in most cancer cell lines, colorectal cancer exhibits decreased TSG expression with DNA hypermethylation (Wang et al., 2024c). Increased expression of DNMTs, as well as their cofactors and readers, is also observed (Wang et al., 2024c). In fact, inhibition of

methyltransferase proteins inhibited growth of colorectal cancer cells (Wang et al., 2024c). Given this, epigenetic-based therapies for colorectal cancer could prove to be extremely fruitful.

2.1.2.1. Caco-2 cell line

Established in the 1970s, the Cancer Coli-2 (Caco-2) cell line originated from the colorectal adenocarcinoma tissue of a 72-year-old Caucasian male. The epithelial adherent cells are commonly used in cancer and toxicology research as they model the intestinal epithelium (Angelis and Turco, 2011).

2.2. Epigenetics and cancer

2.2.1. DNA Methylation

DNA methylation is an epigenetic alteration occurring in mammalian cells that regulates gene expression (Stirzaker et al., 2017). It involves the incorporation of a methyl group (CH_3) onto carbon five of cytosine to produce 5-methylcytosine (5mC) (Figure 2.2.) (Moore et al., 2013). This occurs on cytosine residues that precede guanine, termed CpG islands (Moore et al., 2013). The methyl group is donated from S-adenosyl methionine (SAM) through one-carbon metabolism, during which SAM is transformed into S-adenosyl homocysteine (SAH) (Moore et al., 2013).

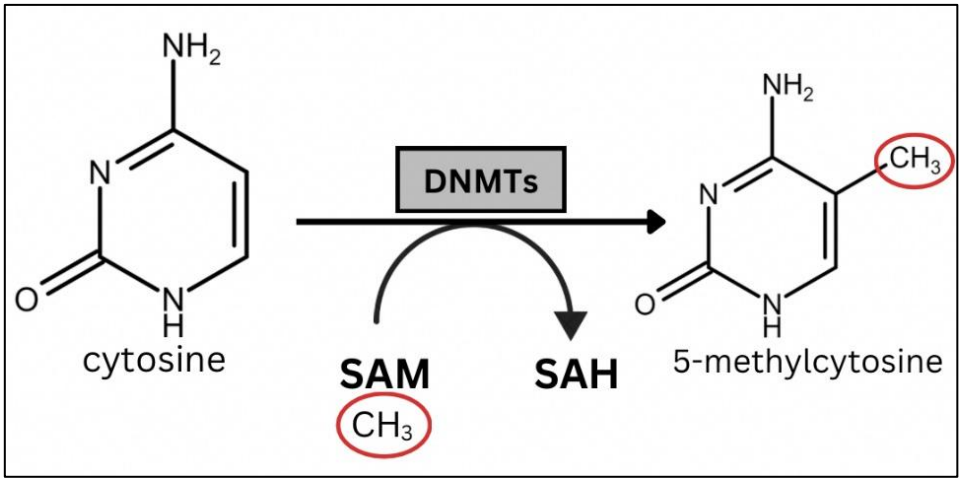

Figure 2.2: Methylation of cytosine to 5-methylcytosine. SAM: S-adenosyl methionine; SAH: S-adenosyl homocysteine (prepared by author).

DNA methylation is carried out by DNA methyltransferases (DNMTs) (Figure 2.2). They contain a regulatory domain and a catalytic domain in their N-terminal and C-terminal, respectively (Gujar et al., 2019). Three subtypes of DNMTs exist: DNMT1, DNMT3a, and DNMT3b. Their expression is regulated by the Sp1 and Sp3 zinc finger proteins (Lin and Wang, 2014). DNMT3a/b are involved in *de novo* methylation, establishing methylation on previously unmethylated DNA (Moore et al., 2013). DNMT1 maintains methylation by copying the methylation pattern from parent strands to daughter strands during DNA replication (Moore et al., 2013).

DNMT1 activity requires the presence of its cofactor UHRF1, an E3 ubiquitin ligase. This protein contains a ubiquitin-like (UBL) domain, tandem tudor domain (TTD), plant homeodomain (PHD), set and ring associated (SRA) domain, and a really interesting new gene (RING) finger domain (Ashraf et al., 2017). UHRF1 binds to hemi-methylated DNA by means of its SRA domain and recruits DNMT1 for maintenance of methylation (Gujar et al., 2019, Sidhu and Capalash, 2017). The RING finger domain of UHRF1 is responsible for its E3 ubiquitin ligase activity. When UHRF1 binds to hemimethylated DNA, it mono-ubiquitinates histone H3 at K18 and K23, which is essential for the recruitment of DNMT1 (Wang et al., 2024a). This ubiquitination allows for the interaction of UHRF1 with the replication focus targeting sequence (RFTS) of DNMT1, thereby recruiting and activating DNMT1 for maintenance of methylation (Wang et al., 2024a).

DNA methylation possesses an inverse relationship with gene expression; promoter methylation down-regulates gene expression (Razin and Kantor, 2005). This occurs for two reasons: (1) methylation directly interferes with transcription factor binding, and (2) the chromatin structure is changed to become inactive heterochromatin (Razin and Kantor, 2005).

Methyl-CpG-binding domain (MBD) proteins act as readers of methylation, facilitating transcriptional silencing through interactions with the nucleosome remodelling deacetylase (NuRD/Mi-2) complex, which consists of the ATP-dependent remodelling enzymes CHD3/4, HDAC1/2, histone chaperones RBBP4/7, and DNA binding proteins GATAD2A/B and MTA1/2/3 (Wood and Zhou, 2016). The MBD2 subtype contains overlapping MBD and transcriptional repression domains (TRD), which alludes to its function in silencing transcription through its methylation-dependent binding to 5mC (Du et al., 2015). Certain transcription factors are methylation-specific; MBD2, bound to the NuRD complex, binds to 5mC and blocks these transcription factors from binding, thereby facilitating transcriptional

repression (Du et al., 2015, Wood and Zhou, 2016). Interestingly, however, MBD2 has also been reported to have demethylase activity *in vitro* and *in vivo* (Detich et al., 2002).

DNA methylation is a reversible process (Figure 2.3). Demethylation employs ten-eleven translocation (TET) proteins for the removal of CH_3 from 5mC. The TET family comprises of TET1, TET2, and TET3 (Kohli and Zhang, 2013). TET proteins achieve their demethylating function by oxidising 5mC to 5-hydroxymethylcytosine (5hmC), 5-formylcytosine (5fC), and 5-carboxylcytosine (5caC) (Wu and Zhang, 2017). 5fC or 5caC are then removed by thymine DNA glycosylase (TDG). The resultant abasic sites are transformed back to cytosine by base excision repair, thereby, restoring gene expression (Wu and Zhang, 2017).

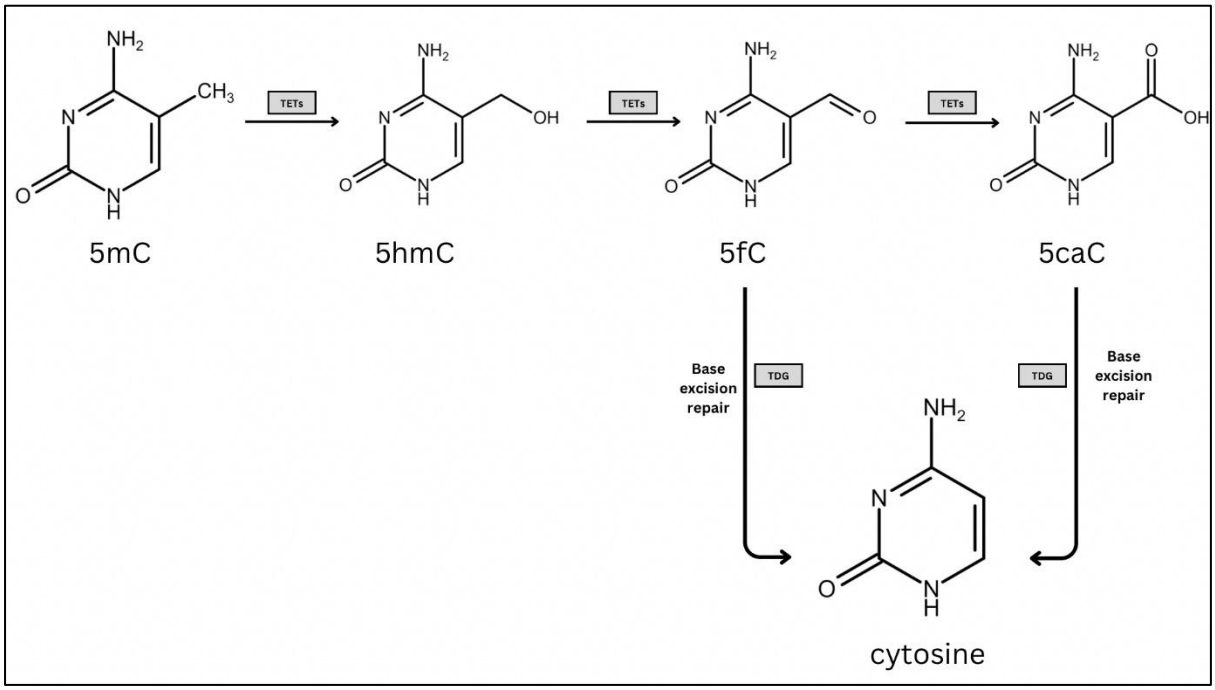

Figure 2.3: The process of demethylation of 5-methylcytosine to cytosine by TET (prepared by author).

2.2.1.1. DNA methylation aberrations in cancer

Aberrant methylation patterns are observed in several types of cancers and tumour cells, making this epigenetic modification a significant hallmark of cancer (Park and Han, 2019). Hypomethylation to increase oncogene expression and hypermethylation to decrease the expression of TSGs are both evident (Chen et al., 2022). Promoter hypermethylation is the most prevalent epigenetic modification observed in tumours (Uddin et al., 2022), with subsequently decreased expression of TSGs and DNA repair genes observed in 5-10% of CpG islands in cancer cells (Chen et al., 2022, Nishiyama and Nakanishi, 2021). In fact, screening

of 98 different types of human tumours revealed approximately 600 abnormally methylated CpG islands in each tumour (Lin and Wang, 2014).

Given the prevalence of hypermethylation, it is not surprising that increased expression of DNMTs is observed in most cancers (Liao et al., 2019), and this is strongly associated with tumorigenesis (Park and Han, 2019). A proposed reason for this phenomenon is that DNA damage by genotoxic stress results in an increase of DNMTs at promotor regions not just at the site of DNA damage, ultimately resulting in transcriptional repression of TSGs (Nishiyama and Nakanishi, 2021). This makes DNMT proteins promising potential targets for the development of anticancer drugs.

Two anti-myelodysplastic syndrome (MDS) drugs that target DNMT1 to cause its degradation have been granted FDA approval; these drugs are azacitidine (5-AZA) and decitabine (Rajendran et al., 2011). 5-AZA is an analogue of cytidine; it functions by incorporating into RNA to inhibit protein synthesis, and incorporating into DNA to reduce the levels of DNMT1. Decitabine is similar to 5-AZA in that it is also a cytidine analogue. However, it only incorporates into DNA to inhibit DNA methylation. *In vitro* inhibition of DNMTs by 5-AZA resulted in upregulation of TSGs in numerous human colon cancer cell lines (Erfani et al., 2022, Fang et al., 2003).

Increased UHRF1 expression is also evident in several cancers (Ashraf et al., 2017), contributing to the hypermethylation state (Sidhu and Capalash, 2017). Knockdown of UHRF1 in several cancer cells reduced methylation, caused reactivation of TSG expression, reduced proliferation, and induced apoptosis (Alhosin et al., 2016, Nishiyama and Nakanishi, 2021, Sidhu and Capalash, 2017).

The methylation reader MBD2 is also overexpressed in cancer cells, including colorectal cancer; this is associated with tumorigenesis (Du et al., 2015, Park and Han, 2019, Wood and Zhou, 2016). It binds to hypermethylated promoters of TSGs to facilitate their silencing (Lopez-Serra et al., 2008). MBD2 knockdown in prostate cancer cells resulted in a loss of methylation maintenance and *de novo* methylation, causing genome-wide hypomethylation (Stirzaker et al., 2017). Knockdown of MBD2 in colon cancer and glioblastomas served to restore TSG gene expression (Zhu et al., 2011, Martin et al., 2008).

Another proposed explanation for the hypermethylation observed in cancer cells is dysregulation of TET proteins (Nishiyama and Nakanishi, 2021). Decreased expression of TET1-3 was observed in several cancers, along with reduced levels of 5hmC (Kohli and Zhang,

2013, Nishiyama and Nakanishi, 2021, Rasmussen and Helin, 2016). This may likely contribute to the high rate of proliferation of tumour cells (Rasmussen and Helin, 2016).

Figure 2.4 summarises the aberrant methylation patterns in cancer.

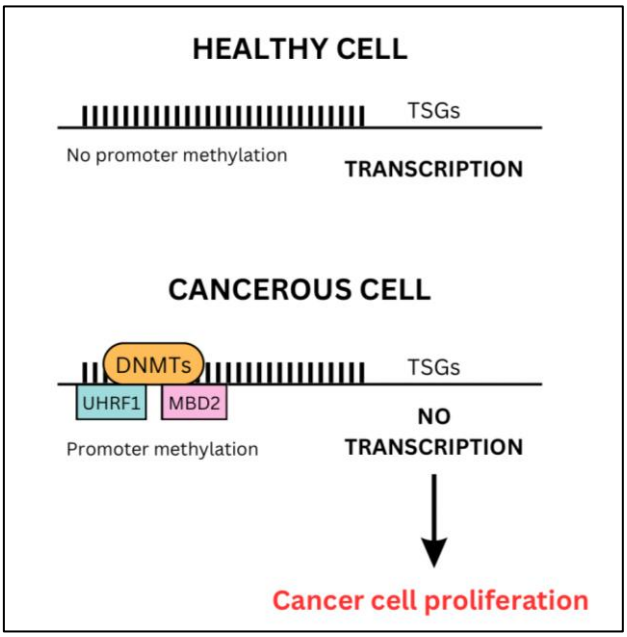

Figure 2.4: DNA methylation aberrations in cancerous cells. TSG: tumour suppressor genes; DNMTs: DNA methyltransferases; UHRF1: ubiquitin-like containing PHD and RING finger domains 1; MBD2: methyl-binding domain 2 (prepared by author).

2.2.2. MicroRNAs

MicroRNAs (miRNAs) are small non-coding RNA molecules that are responsible for the negative regulation of gene expression at the post-transcriptional stage (Bushati and Cohen, 2007). They interact with the 3' untranslated regions (3'UTRs) of target mRNA sequences by complementary base pairing to repress gene expression (Bushati and Cohen, 2007). This binding prevents translation of the target mRNA or causes its degradation (Garcia-Lopez et al., 2013). Individual miRNAs can target several mRNAs to affect gene expression (Lu and Rothenberg, 2018). miRNAs regulate the expression of approximately 60% of mammalian genes (Garcia-Lopez et al., 2013). Dysregulated miRNA expression results in several diseases such as cancer (Ali Syeda et al., 2020), neurodegenerative conditions (Quinlan et al., 2017), cardiovascular disease (Wronska, 2023), and diabetes (Bahreini et al., 2022).

2.2.2.1. Canonical pathway of miRNA biogenesis

The canonical pathway begins in the nucleus, where primary miRNAs (pri-miRNA) several hundred nucleotides long are transcribed by RNA polymerase II (Bhaskaran and Mohan, 2014). The enzyme Drosha dimerises with DiGeorge syndrome critical region gene 8 (DGCR8) to form a microprocessor complex, which cuts pri-miRNAs into shorter hairpin-structured precursor miRNAs (pre-miRNAs) (Bhaskaran and Mohan, 2014). These are then transported out of the nucleus by the Ran-GTP-dependent nuclear transport receptor protein, Exportin 5.

The next phase occurs in the cytoplasm, where the RNase III enzyme Dicer-1 processes the pre-miRNAs into mature double-stranded miRNA duplexes (Bhaskaran and Mohan, 2014). The strands separate; one strand (characterised by unstable base pairing at the 5' end) serves as the guide strand and is deposited onto Argonaute (AGO) proteins to form the RNA-induced silencing complex (RISC) (Bhaskaran and Mohan, 2014). The other strand (with stable base pairing at the 5' end) is usually degraded (Bhaskaran and Mohan, 2014). The RISC uses the guide strand to complementary bind to target mRNA, leading to repressed gene expression by either preventing translation or causing mRNA degradation (Garcia-Lopez et al., 2013).

2.2.2.2. Non-canonical pathway of miRNA biogenesis

The non-canonical pathway occurs independent of Drosha/DGCR8 or Dicer (Bushati and Cohen, 2007, Matsuyama and Suzuki, 2019). Examples are mirtrons, tailed mirtrons, tRNA fragments, and snoRNA fragments, (Matsuyama and Suzuki, 2019). Mirtrons formed from mRNA introns are processed into pre-miRNAs by spliceosomes, independent of Drosha/DGCR8 (Garcia-Lopez et al., 2013). The pre-miRNAs are bound to Exportin 5 and transported to the cytoplasm to continue the canonical pathway (Garcia-Lopez et al., 2013). tRNAs produce miRNAs that require splicing by Dicer (Garcia-Lopez et al., 2013). snoRNAs generate miRNAs that are processed by Dicer, independent of Drosha/DGCR8 (Garcia-Lopez et al., 2013).

2.2.2.3. miR-29

There are three key players in the miR-29 family: miR-29a, 29b, and 29c (Kwon et al., 2019). All three possess a significant role in cancer epigenetics and are downregulated in the majority of cancers (Jiang et al., 2014). However, they are highly expressed in normal tissues (Jiang et al., 2014).

The miR-29 family act as tumour suppressors and directly down-regulate DNMT3a/b expression in several cancers (Kwon et al., 2019). miR-29b has proven to indirectly down-regulate DNMT1 by targeting its transcription factor Sp1 (Garzon et al., 2009). Enforced expression of miR-29 in Burkitt lymphoma cells reduced DNMT3b expression as well as cell proliferation (Mazzoccoli et al., 2018). Similarly, enforced expression in lung cancer cells reduced DNMT3a/b expression and induced apoptosis (Fabbri et al., 2007).

2.3. Thymoquinone

2.3.1. NS

Nutritious diets play an influential role in sustaining a healthy lifestyle and are strongly linked to average life expectancy. Extensive research is conducted to investigate the health benefits of plant-based foods. Among these foods, herbs and spices used for flavouring have proven to possess great health benefits and therapeutic potential against numerous diseases (Hannan et al., 2021). Drugs derived from natural sources constitute a large part of pharmaceuticals available in modern medicine, with research continually being conducted in this field (Kubczak et al., 2021).

Thymoquinone (TQ), derived from the essential oil of the herb *Nigella sativa* (NS), is one such compound that has become a recipient of great attention for its promising therapeutic capacity. NS, generally called black cumin, is a herb belonging to the *Ranunculacae* family (Ahmad et al., 2013). It is found largely in the Mediterranean region, Northern Africa, and India, and has been used in these regions for culinary and medicinal purposes for hundreds of years (Hannan et al., 2021). Historically, NS has been given great importance for its mentions in Islamic and Christian texts. Muslims know it as the “prophetic medicine” due to claims in Islamic records that the herb contains a cure for every disease except death, and the Bible refers to NS as “curative black cumin” (Ahmad et al., 2013).

NS is used in several forms; the most common being as an oil, paste, powder, or pure seed extract (Hannan et al., 2021). It has been used for the treatment of various conditions, including but not limited to hypertension, diabetes, influenza, gastrointestinal problems, skin conditions, asthma, bronchitis, inflammatory diseases, neurological problems, and cancer (Sarkar et al., 2021). It also exhibits potent antioxidant, anti-obesity, cardio-protective, hepato-protective, and nephroprotective effects (Dalli et al., 2021).

The monoterpene compound TQ is the main bioactive compound of NS and is largely responsible for the herb's therapeutic effects (Malik et al., 2021). Other components of NS are thymohydroquinone, thymol, carvacrol, nigellidine, nigellicine, and α-hederin (Hannan et al., 2021). The herb also contains vital nutrients such as proteins, fats, essential fatty acids, vitamins, and minerals (Kooti et al., 2016).

2.3.2. TQ

Thymoquinone is the primary constituent of NS that is responsible for most of its therapeutic effects. However, it is not only found in NS, but also in the flowering portions of *Thymus vulgaris*, the leaves of the Origanum species, and the essential oil from *Calocedrus decurrens* (Malik et al., 2021). Isolated TQ displays antioxidant, anti-inflammatory, anti-microbial, anti-convulsant, and a host of other therapeutic effects (Goyal et al., 2017). It also exhibits neuroprotective, cardioprotective, hepatoprotective, nephroprotective, and hypoglycaemic properties (Alam et al., 2022). However, the most widely studied are its anti-cancer effects, which are discussed below.

2.3.2.1. Chemical properties

The compound TQ (molecular weight: 164,20 g/mol) was first isolated in the year 1960 by El-Dakhakhany (Schneider-Stock et al., 2014). It is a yellow crystal-like substance that is soluble in ethanol, dimethyl sulfoxide, and dimethyl formamide (Malik et al., 2021). It is stable in lower pH solutions and displays decreasing stability as pH increases (Malik et al., 2021). Figure 2.5 depicts its chemical structure, which consists of a basic quinone ring with two carbon-oxygen and two carbon-carbon double bonds. TQ exhibits low lipophilicity; however, the incorporation of an alkyl chain has been shown to enhance its lipophilicity (Antonenko et al., 2008).

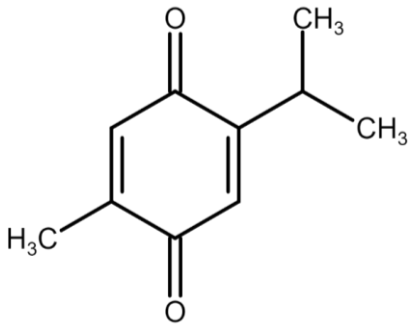

Figure 2.5: Chemical structure of thymoquinone (2-isopropyl-5-methyl-1,4-benzoquinone; $C_{10}H_{12}O_2$). Chemical structure was drawn by author using RCSB PDB Chemical Sketch Tool.

2.3.2.2. Pharmacokinetics and toxicity of TQ

Given the poor lipophilicity of TQ, it is expected that the compound would display less than stellar bioavailability. A study investigating its pharmacokinetics in Vole rabbits revealed an absolute bioavailability of 58% with rapid elimination (Alkharfy et al., 2015). Intravenous and oral administration were 5 mg/kg and 20 mg/kg, respectively. With intravenous administration, volume of distribution was 700,90 ± 55,01 mL/kg, clearance was 7,19 ± 0,83 mL/kg/min, and the elimination half-life was 63,43 ± 10,69 min. Oral administration displayed a clearance of 12,30 ± 0,30 mL/kg/min, volume of distribution of 5109,46 ± 196,08 mL/kg, and an elimination half-life of 274,61 ± 8,48 min. Thus, it is clear that TQ displays slow absorption after oral administration (Alkharfy et al., 2015). Its low bioavailability may be circumvented by applying nanotechnology-based systems of drug delivery (Asaduzzaman Khan et al., 2017).

Insufficient data is available on the metabolism and excretion of TQ. It may undergo biotransformation in the gastrointestinal tract to form less toxic metabolites, or metabolism in the liver to dihydrothymoquinone (Hannan et al., 2021). Following this, elimination is rapid. However, the exact mechanisms remain unclear.

The toxicity of TQ depends on the dosage, route of administration, and duration of exposure (Hannan et al., 2021). A study investigating its toxicity in mice compared oral and intraperitoneal administration (Al-Ali et al., 2008). The LD_{50} (lethal dose) with intraperitoneal administration was 104,7 mg/kg, which was 10-15 times greater than the minimum effective dose. Oral administration displayed an LD_{50} of 870,9 mg/kg: a value 100-150 times greater than the minimum effective dose. This reveals a wide therapeutic window, with oral administration being significantly safer than intraperitoneal administration. Its minimal toxicity provides a basis for the historical use of TQ in food and for medicinal purposes.

2.3.2.3. Molecular mechanisms of the anti-cancer effects of TQ

TQ exhibits a vast array of therapeutic effects by targeting several biochemical signalling pathways. The most notable are the Nrf2, Nf-κB, TLR, PI3K/Akt, SIRT1, PPAR, AMPK-SIRT-1-PGC-1α, and mTOR pathways (Hannan et al., 2021). Through interactions with several key players, TQ exerts effects such as reducing oxidative stress (Nrf2), inhibiting inflammation (Nf-κB and TLR), preventing or inducing apoptosis (PI3k/Akt), inducing autophagy (SIRT1), and affecting energy metabolism (PPAR and AMPK-SIRT-1-PGC-1α) (Hannan et al., 2021). The anticancer effects of TQ are the most widely studied; it induces cell cycle arrest and

apoptosis through various signalling pathways, as well as affecting oxidative stress, metastasis, and angiogenesis. The effects of TQ on glioblastoma and other types of cancers are summarised below, as well as its epigenetic effects.

2.3.2.3.1. Colon cancer

An *in vitro* study using human colon cancer cells (LoVo) displayed reduced proliferation and inhibition of metastasis through upregulation of JNK and p38, and downregulation of PI3K and NF-κB signalling following 24 hours exposure to TQ (2, 4, 6, and 8 μM) (Chen et al., 2017). A similar study (18 hours exposure to 60 μM TQ) revealed reduced c-Myc, Bcl-2, and VEGF expression (Zhang et al., 2016). Concurrent exposure to TQ (40 μM for 24 hours) and the chemotherapeutic drug Topotecan (0.6 μM for 24 hours) displayed a synergistic effect; reduced tumour cell proliferation and increased p53 and Bax were observed, with reduced Bcl-2 expression (Khalife et al., 2016).

An *in vivo* study using Wistar rats concurrently exposed to TQ (5 mg/kg daily for 14 days) and the drug 5-fluorouracil (50 mg/kg on day 15) also revealed a synergistic effect with decreased tumour growth (Eftekhar et al., 2022). Interestingly, a similar study using rat models with induced colorectal cancer revealed decreased expression of precancerous genes and increased anti-tumorigenesis gene expression following administration of TQ (35 mg/kg/day, 3 days/week in week 7 and 15 post-induction) and 5-fluorouracil (12 mg/kg/day for four days, followed by 6 mg/kg/day every alternate day for four more doses in week 9 and 10) (Kensara et al., 2016).

2.3.2.3.2. Breast cancer

In vitro studies using human breast cancer cells (Mcf7) revealed that TQ (100 μM for 24 or 48 hours) induced apoptosis through upregulation of p53, p21, Bax, cleaved PARP and caspases (Arafa el et al., 2011). TQ also decreased Bcl-xl and Bcl-2 activity and induced cell cycle arrest (1–25 μM TQ for 24–72 hours) (Sutton et al., 2014).

In mice models with breast cancer, administration of TQ (20 and 100 mg/kg every three days) decreased tumour growth and inhibited metastasis through inhibition of eEF-2K expression (Kabil et al., 2018). Apoptosis was induced in chick embryo models inoculated with breast cancer through increased p53 and Bax and decreased Bcl-2 expression following concurrent treatment with TQ and Emodin (1/15 μg/ml on day 10 and 12 after inoculation) (Bhattacharjee et al., 2020).

2.3.2.3.3. Bladder and kidney cancer

Similar to breast and colon cancer, TQ induced apoptosis in bladder (40-80 μM TQ for 24 hours) and kidney cancer (40 and 50 μM TQ for 24 hours) cells (Dera and Rajagopalan, 2019, Zhang et al., 2018a). Inhibited proliferation and metastasis were observed in human bladder cancer cells through downregulation of Myc, MET, and cyclin-D1 following 20 and 40 μmol/l TQ exposure for 24 hours (Zhang et al., 2020b). Interestingly, autophagy was detected in human renal cancer cells with increased AMPK/mTOR signalling following treatment with TQ (40 μmol/l for 24 hours) (Zhang et al., 2018b).

2.3.2.3.4. Lung cancer

Apoptosis was also observed in human lung cancer cells following treatment with TQ (25-100 μM for 24 or 48 hours), with upregulation of p53 and increased activity of caspases 3 and 9 (Samarghandian et al., 2019). Inhibition of metastasis was evident through decreased ERK1/2 signalling as well as cell cycle arrest through reduced expression of cyclin-D1 following treatment with 5-160 μmol/l TQ for 24, 48, or 72 hours (Yang et al., 2015).

Similar to *in vitro* studies, an investigation conducted on lung cancer in mice revealed induction of apoptosis by means of increased p53, increased Bax, and decreased Bcl-2 expression following administration of 20 mg/kg TQ for eight weeks (Hussein et al., 2016).

2.3.2.3.5. Liver cancer

An *in vitro* study using human hepatocellular carcinoma cells (HepG2) revealed cell cycle arrest and increased apoptosis through upregulation of caspase-3 and caspase-9, cleaved PARP, increased Bax, and decreased Bcl-2 following exposure to 12.5-100 μM TQ for 6-24 hours (Ashour et al., 2014).

In vivo studies displayed similar results. A study conducted on hepatocellular carcinoma in Wistar rat models administered 20 mg/kg TQ thrice a week for 16 weeks revealed a reduction in cell proliferation with decreased Bcl-2 expression and increased antioxidant (GSH, GST, SOD) activity (Shahin et al., 2018). Sprague Dawley rats with hepatocellular carcinoma displayed increased apoptosis with increased caspase-3 and decreased Bcl-2 expression, along with increased expression of TRAIL1/2 genes following oral administration of TQ (20 mg/kg daily for 16 weeks) (Helmy et al., 2019).

2.3.2.3.6. TQ and epigenetic alterations in cancer cells

Limited information exists regarding the effects of TQ on epigenetic machinery in cancers, but the information that is available is extremely promising. TQ has been shown to interact with several epigenetic players, namely DNMTs, UHRF1, TETs, and certain miRNAs. No information is available with regard to the effects of TQ on these players in colon cancer; however, its effects on several other cancers are described below.

A study conducted on leukaemia cells revealed that 24 hours exposure to 3 and 10 μM TQ decreased DNMT1 expression by causing the dissociation of its transcription factor complex Sp1/Nf-κB from its promoter region (Pang et al., 2017). This resulted in increased apoptosis through upregulated caspase expression. Another study involving acute lymphoblastic leukaemia cells (Jurkat) revealed that exposure to 5-20 μM TQ for 24 hours reversed the epigenetic silencing of several TSGs through downregulation of DNMT1, DNMT3a, and DNMT3b (Qadi et al., 2019). Subsequently, TSGs and pro-apoptotic genes were upregulated, indicating the occurrence of apoptosis. Treatment of myeloid leukaemia cells with 5.5 μM and 15 μM TQ for 48 hours caused decreased DNMT1, DNMT3a, and DNMT3b expression as well as increased TET2 expression (Al-Rawashde et al., 2021, Al-Rawashde et al., 2023). This restored SHP-1 and SOCS-2 expression, both of which are silenced by hypermethylation in cancer. JAK/STAT signalling, which is negatively regulated by SHP-1 and SOCS-3, was subsequently downregulated, inducing cell cycle arrest and apoptosis. Concurrent exposure of liver cancer and breast cancer cells to TQ (31.57 μM and 29.92 μM, respectively, for 24 hours) and the drug Sorafenib revealed a synergistic effect: DNMT3B expression was reduced, restoring normal expression of TSGs (El-Shehawy et al., 2023). Interestingly, molecular dynamics analysis of the interaction between TQ and DNMT1 showed that TQ interacts with the catalytic domain of DNMT1, competing with SAM and inhibiting the methyltransferase activity (Pang et al., 2017).

Phosphodiesterases (PDEs) hydrolyse the molecules cAMP and cGMP, both of which are involved in several signalling pathways. Inhibition of PDEs results in cell cycle arrest and apoptosis through the p73 pathway. Jurkat cells displayed downregulation of PDE1A as well as UHRF1 through p73 upregulation following exposure to 10 and 20 μM TQ for 24 hours (Abusnina et al., 2011). Another mechanism by which TQ inhibits UHRF1 activity is through HAUSP, which de-ubiquitinates UHRF1 and protects it from degradation. Exposure to 1-30 μM TQ for 24 hours downregulated HAUSP in Jurkat and HeLa cells resulting in UHRF1

histone poly-auto-ubiquitination, caspase-3 activation, and apoptosis (Ibrahim et al., 2018). Jurkat cells exposed to TQ (10 µM for 24 hours) in combination with difluoromethylornithine (DFMO) displayed significantly downregulated UHRF1 and DNMT1 activity, with upregulated TSG expression (Alhosin et al., 2020).

3 hours exposure to 10 µM TQ upregulated miR-29 expression in leukaemia cells causing tumour suppressor effects (Homayoonfal et al., 2021, Pang et al., 2017). 24 hours exposure to 3 and 10 µM TQ resulted in blocked PI3K/Akt signalling, which activated caspase-3 and caspase-8, ultimately resulting in apoptosis. KIT and FLT tyrosine kinases were inactivated, causing subsequent inactivation of STAT5 and reduced tumour growth. Finally, miR-29b split the Sp1/Nfκ-B complex, causing its dissociation from the DNMT1 promoter region; this reduced the hypermethylation that is evident in cancer, and induced apoptosis (Pang et al., 2017).

Figure 2.6 summarises the epigenetic effects of TQ in cancerous cells.

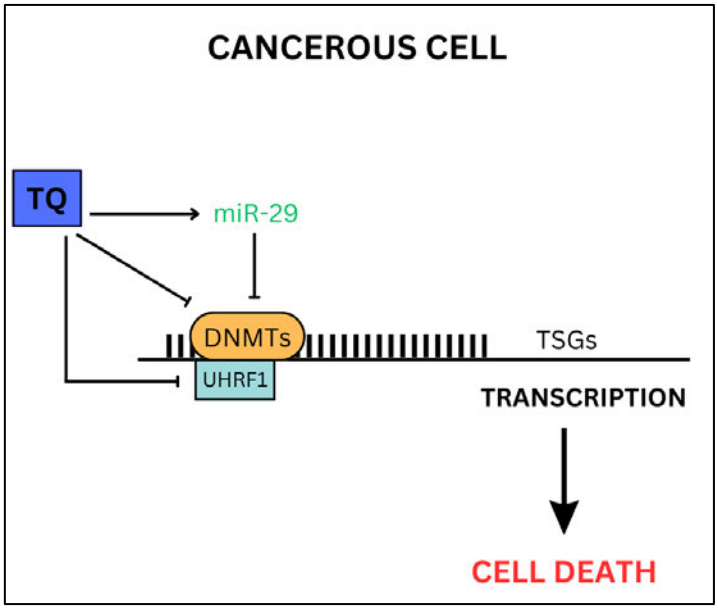

Figure 2.6: Thymoquinone ameliorates DNA methylation alterations in cancer cells (prepared by author).

2.3.2.4. Clinical trials

The anticancer effects of TQ in humans are still largely unexplored. A clinical trial investigating TQ's effects on various kinds of advanced refractory malignant disease has been completed (Kurowska et al., 2023). The trial consisted of 21 adult patients who were divided into three groups, each of which received varying doses of TQ daily (3 mg/kg, 7 mg/kg, and 10 mg/kg)

with the doses increasing weekly for up to 20 weeks. No toxicities were observed for doses up to 2600 mg/day. Decreased tumour markers were observed, but less than 25% of the baseline amount. Another clinical trial investigating the effects of TQ against oral potentially malignant lesions in 30 adult patients is still ongoing (Phua et al., 2021).

Other non-cancer-related clinical trials that are still ongoing regard acne vulgaris, arsenical keratosis, and Covid-19 (Phua et al., 2021).

2.3.2.5. Limitations of TQ for cancer treatment

TQ displays low bioavailability due to its poor lipophilicity, which remains a limitation when considering it for anticancer treatment. Encapsulating TQ in nanoparticles to improve its delivery has shown promising anticancer results *in vitro* and increased bioavailability *in vivo* (Phua et al., 2021). Examples of nanoparticle carriers are lipid-based, chitosan-based, liposomal, and polymeric carriers (Ballout et al., 2018).

CHAPTER 3: MATERIALS AND METHODS

3.1. MATERIALS

Caco-2 cells were sourced from Separations Scientific (Johannesburg, South Africa), while reagents used for cell culture were obtained from Whitehead Scientific (Johannesburg, South Africa). TQ (purity: ≥ 98%) was procured from Merck (Darmstadt, Germany). Reagents for Western Blot were supplied by Bio-Rad (Hercules, CA, USA), and a colorimetric DNA methylation quantification kit was purchased from Abcam (Cambridge, UK). Unless specified otherwise, all other reagents were obtained from Merck (Darmstadt, Germany).

3.2. CELL CULTURE AND TREATMENT

Caco-2 cells were cultured at 37°C with 5% CO_2 in 25 cm^3 cell culture flasks containing Dulbecco's Modified Eagle Medium (DMEM) with 2.5% HEPES buffer, 1% penicillin-streptomycin-fungizone, 1% L-glutamine, and 10% foetal calf serum (FCS). Penicillin-streptomycin-fungizone is an antibiotic and fungicide that prevents bacterial and fungal contamination (Martinez-Liarte et al., 1995). FCS contains a cocktail of growth-enhancing molecules such as proteins, vitamins, hormones, and growth factors (Fang et al., 2017). Glutamine is an essential nutrient for cells, and supports cell growth and differentiation (Heeneman et al., 1993). Most mammalian cultured cells cannot survive in an environment without glutamine (Zhang et al., 2017).

A TQ stock solution (100 mM) was made up in 100% dimethyl sulfoxide (DMSO) and was diluted in DMEM for use in all assays. An untreated control (DMEM only) was also prepared, as well as a DMSO control containing the same volume of DMSO as the TQ treatment. At 80% confluency, the cells were incubated with DMEM, TQ, or DMSO for 24 hours.

3.3. 3-(4,5-DIMETHYLTHIAZOL-2-YL)-2,5 DIPHENYL TETRAZOLIUM BROMIDE (MTT) ASSAY

3.3.1. Introduction

The MTT assay was employed to determine the impact of TQ on the viability of Caco-2 cells by measuring mitochondrial activity. This assay relies on mitochondrial reductases in viable cells that convert the yellow MTT salt to a purple formazan product (Figure 3.1) (Prabst et al., 2017). The intensity of the purple colour is in direct proportion to cell viability. The resulting

formazan crystals are solubilised by DMSO, and absorbance is measured at 570 nm, with 690 nm set as the reference wavelength.

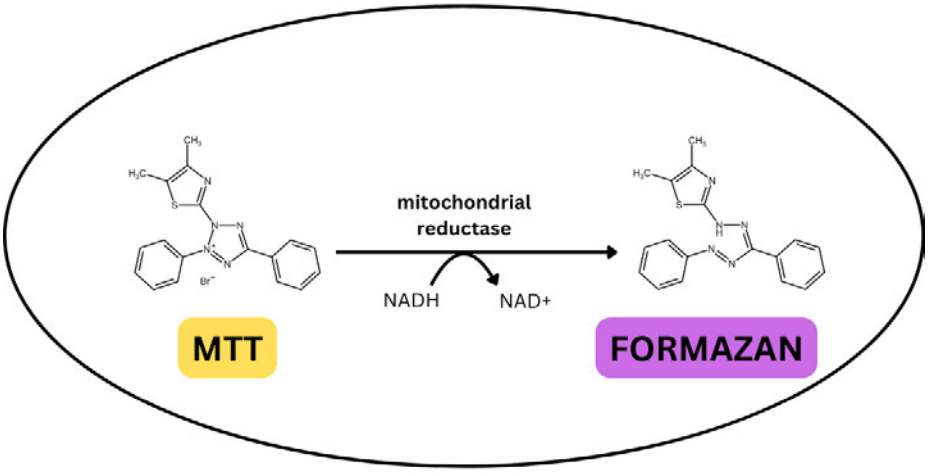

Figure 3.1: Conversion of the yellow MTT salt to a purple formazan product by mitochondrial reductases in viable cells (prepared by author).

3.3.2. Protocol

Caco-2 cells (15 000 cells per well) were seeded in a 96-well microtiter plate overnight before incubation (37°C) with TQ at various concentrations (0-800 µM) for 24 h. Following incubation, the MTT salt solution was prepared (5 mg/mL in 0.1 M PBS) and 20 µL was added to each well, along with 100 µL of DMEM. The plate was incubated for 4 h at 37°C. Afterwards, the MTT solution was discarded, and the formazan crystals were solubilised with DMSO (100 µL per well). The plate was incubated again at 37°C for 1 h, and the absorbances were read spectrophotometrically (570 nm; reference wavelength of 690 nm) using a Biotek µQuant Plate reader (Winooski, VT, USA).

Cell viability was assessed with the following equation:

$$\%\ \text{cell viability} = \frac{\text{treated sample absorbance (average)}}{\text{untreated control absorbance (average)}} \times 100$$

GraphPad Prism v5.0 was used to plot the results as log concentration against percentage cell viability, and the IC_{50} concentration was determined for use in all subsequent assays.

3.4. PROTEIN ISOLATION

3.4.1. Introduction

CytoBuster™ reagent (Novagen, USA), supplemented with protease and phosphatase inhibitors, is used to extract proteins from cells. It is a mild reagent designed to lyse cell membranes to allow efficient extraction of proteins. Supplementation with protease and phosphatase inhibitors protects the proteins from degradation during extraction (Ryan and Henehan, 2017). The protein isolation process is conducted on ice to protect the protein from degradation.

The bicinchoninic acid (BCA) assay (Figure 3.2) is used for the quantification of crude protein and relies on the Biuret reaction . Cu^{2+} ions in an alkaline medium react with peptide bonds in a given sample and are reduced to Cu^{+} (Cortes-Rios et al., 2020). Two molecules of BCA then bind to one Cu^{+} ion to form an intense, purple-coloured chromophore complex. The intensity of the resulting colour increases proportionally with the protein concentration.

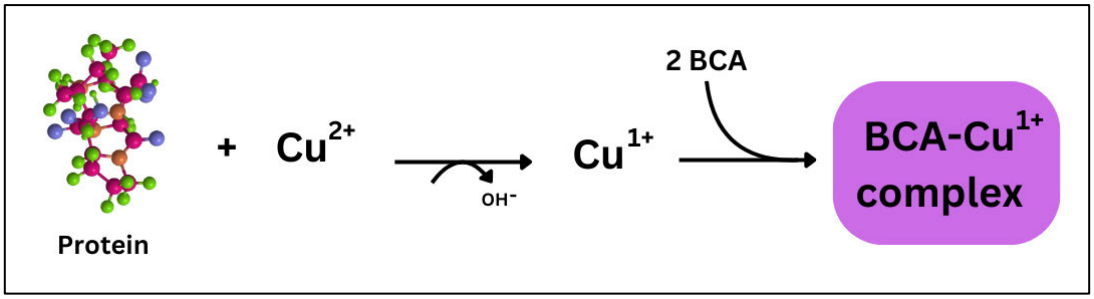

Figure 3.2: The principle of the BCA assay, in which Cu^{+} (formed by the reaction between Cu^{2+} and peptide bonds in the protein sample) reacts with BCA to produce a purple-coloured complex (prepared by author).

3.4.2. Protocol

3.4.2.1. Protein isolation

Control and treated Caco-2 cells were washed thrice with 0.1 M PBS, after which 200 µL of CytoBuster reagent was added. The flasks were left on ice for 30 min, followed by mechanical cell lysis with a cell scraper. The homogenates were carefully pipetted into 1.5 mL micro-centrifuge tubes and subjected to centrifugation (13 000 x g, 10 min, 4°C). The protein supernatants were stored at -80°C for further procedures.

3.4.2.2. Quantification and standardisation of protein samples

The protein standard bovine serum albumin (BSA) was used to quantify protein. Serial dilutions of BSA (0, 0.2, 0.4, 0.6, 0.8, and 1 mg/mL) were prepared in distilled water. Standards

and protein samples (25 µL each) were added to designated wells of a 96-well plate, following which a BCA solution (200 µL; 198 µL BCA and 4 µL $CuSO_4$) was added. The plate was incubated (30 min, 37°C), and absorbances were measured spectrophotometrically at 562 nm.

A standard curve was constructed, and the protein concentration of each sample was determined by extrapolation. The samples were standardised with CytoBuster reagent to the lowest sample concentration (0.35 mg/mL) for the Western blot assay.

3.5. WESTERN BLOTTING

3.5.1. Introduction

3.5.1.1. Sample preparation

Standardised protein samples were prepared for separation with the addition of Laemmli buffer, which is composed of Tris-HCl, bromophenol blue, β-mercaptoethanol, glycerol, and sodium dodecyl sulphate (SDS). Each component of the buffer serves a specific purpose to ensure effective separation (Hnasko and Hnasko, 2015). Tris-HCl prevents changes in the pH of the sample solution. Bromophenol blue is a dye that allows visualisation of the protein samples during migration. β-mercaptoethanol breaks disulphide bonds, causing denaturing of the proteins to their primary structure. Glycerol adds weight to the samples, allowing it to sink into the gel. SDS alters the inherent charges of the proteins, giving all samples a negative charge to ensures that protein separation occurs solely by size.

Once the Laemmli buffer is added, the samples are heated to activate the β-mercaptoethanol and SDS to facilitate denaturation and reduction of the proteins (Mahmood and Yang, 2012).

3.5.1.2. SDS-PAGE

Sodium dodecyl sulphate polyacrylamide gel electrophoresis (SDS-PAGE) exploits the negative charge of proteins to separate them according to their molecular weights: the negatively charged proteins migrate through the polyacrylamide gel towards the positive electrode (Hnasko and Hnasko, 2015). The molecular weight of the proteins affects their rate of migration: larger proteins migrate more slowly, while smaller proteins move faster (Hnasko and Hnasko, 2015).

The gels used in SDS-PAGE are composed of acrylamide, N, N'-methylene bis-acrylamide, tetra-methylethylenediamine (TEMED), and ammonium persulfate (APS). TEMED and APS act as catalysts for the polymerisation and cross-linking of the gel. Two polyacrylamide gels are employed in SDS-PAGE: a stacking gel and a resolving gel. The stacking gel, with a lower

acrylamide concentration, has larger pores, resulting in weak separation of proteins; however, the stacking gel is important in arranging the proteins into linear bands (Mahmood and Yang, 2012). In contrast, the resolving gel, with a higher concentration of acrylamide, has narrower pores, allowing for better protein separation based on size. Smaller proteins pass through the narrower pores more quickly, thus traveling further down the gel.

3.5.1.3. Western blotting

Western blotting is a technique used to detect and quantify specific proteins based on antigen-antibody interactions (Figure 3.3) (Mahmood and Yang, 2012). Once separated by electrophoresis, the proteins are transferred onto a nitrocellulose membrane by means of an electric charge. This process also exploits the negative charge of the proteins: a gel-nitrocellulose membrane sandwich is prepared between two electrodes and a perpendicular charge is applied (Mahmood and Yang, 2012). The proteins migrate towards the positive electrode, transferring from the gel to the membrane.

The membrane is then blocked to prevent non-specific protein binding, followed by incubation with specific antibodies. Primary antibodies bind to the protein of interest, and enzyme-conjugated secondary antibodies bind to the primary antibody to ensure accurate detection (Hnasko and Hnasko, 2015). The target protein is visualised through a reaction between the secondary antibody and a substrate solution containing hydrogen peroxide (H_2O_2) and luminol. H_2O_2 reacts with the enzyme-conjugated secondary antibody to generate free oxygen radicals, which in turn react with luminol to produce aminophthalic acid (Hnasko and Hnasko, 2015). This reaction produces luminescence, the strength of which is directly related to the amount of protein expressed.

A housekeeping protein is used for the normalisation of protein expression (Mahmood and Yang, 2012). They act as loading controls to ensure accurate results and are highly expressed in all cell types. Examples of generally used housekeeping proteins are β-actin and GAPDH.

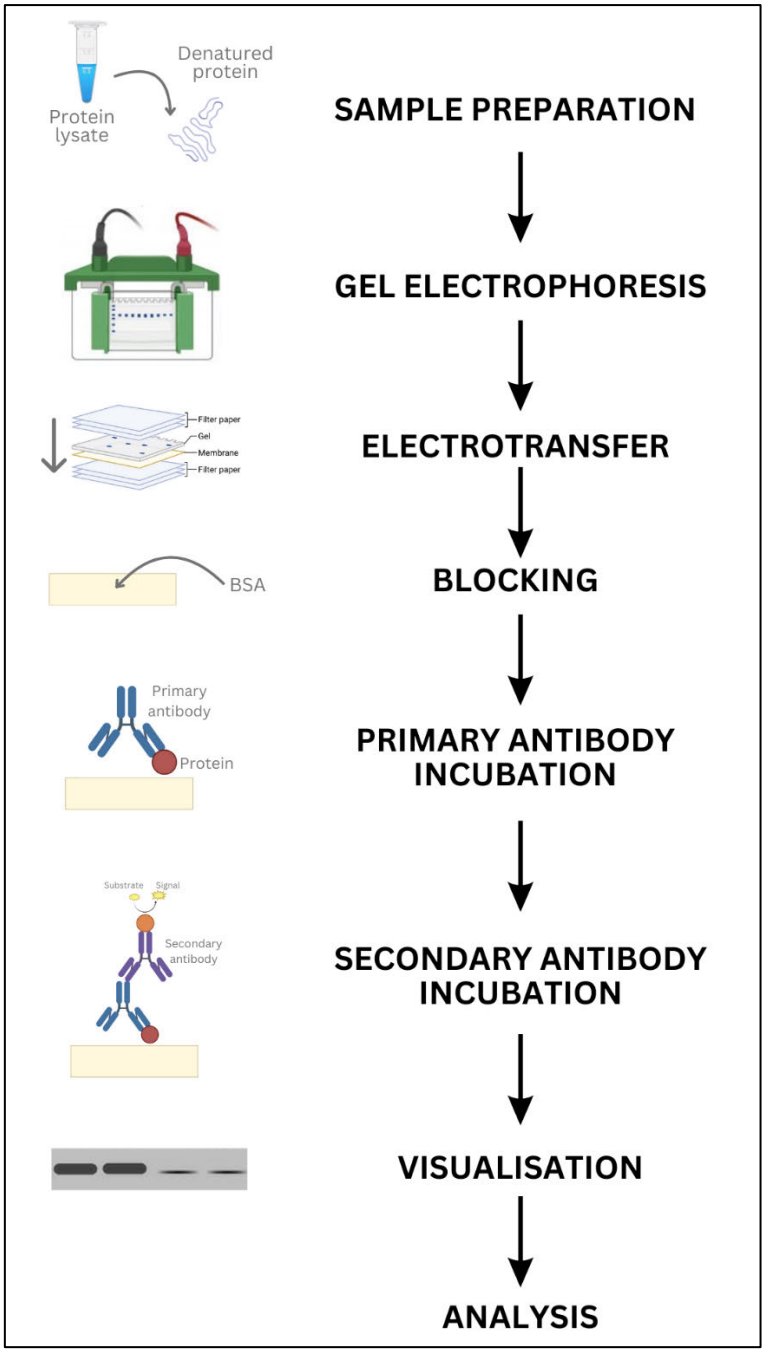

Figure 3.3: Overview of Western blotting protocol (prepared by author).

3.5.2. Protocol

3.5.2.1. Sample preparation

50 µL of Laemmli buffer was added to the standardised protein samples. The samples were heated (100°C) for 5 min, then cooled at RT (~24 - 28°C) before SDS-PAGE.

3.5.2.2. SDS-PAGE

The Mini-PROTEAN 3 SDS-PAGE apparatus (Bio-Rad) was assembled, and a 10% resolving gel (dH_2O, 1.5 M Tris, SDS, bis-acrylamide, APS, TEMED) was prepared and added to the

apparatus. Once set, the 4% stacking gel (dH_2O, 0.5 M Tris, SDS, bis-acrylamide, APS, TEMED) was poured on top, and a Bio-Rad comb was inserted into the stacking gel to form wells for loading the samples. The gel was allowed to set at RT for 1 h.

The set gels were assembled in the electrode tank for electrophoresis. The samples (30 µL) and molecular weight markers (5 µL) were loaded into their predesignated wells and the tank was filled with running buffer (SDS, Tris, glycine). Electrophoresis was carried out using the Bio-Rad compact power supplier (150 V, 1 h).

3.5.2.3. Electro-transfer

Following SDS-PAGE, the gels were equilibrated in transfer buffer (glycine, methanol, Tris; pH 8.3) and a gel sandwich comprising of two fibre pads, a nitrocellulose membrane, and the electrophoresed gel was assembled. The gel sandwich was placed between two electrodes, and a Bio-Rad Trans-Blot Turbo Transfer System was used to transfer the proteins to the membrane (25 V, 30 min).

3.5.2.4. Immunoblotting and visualisation

The membranes were blocked with 5% BSA (1 hr, RT) then incubated with primary antibodies (Table 1) overnight at 4°C. After incubation, the membranes were washed with TTBS, then incubated with horseradish peroxidase-conjugated secondary antibodies [goat anti-rabbit (Cell Signalling Technology, 7074S) and goat anti-mouse (Cell Signalling Technology, 7076P2)] with gentle shaking at RT (2 h, 1: 5 000 in 5% BSA). Following this, the membranes were washed five times with TTBS, and the protein bands were visualised using the Bio-Rad Clarity Western ECL Substrate Kit and the iBright™ CL1500 Imaging System (Thermo-Fisher Scientific). The iBright™ Analysis Software v4.0 (Thermo-Fisher Scientific) was used for analysis of images.

3.5.2.5. Normalisation

The membranes were stripped of antibodies with 5% H_2O_2 (30 min, 37°C), then washed once with TTBS (10 min, RT). The membranes were subsequently blocked with 5% BSA, incubated with anti-β-actin (Sigma-Aldrich, A3854; 1:5 000) for 30 min at RT, washed with TTBS (10 min, RT), then visualised. Results were presented as the relative change in band density (RBD) normalised to β-actin.

Table 1: Primary antibody dilutions

Antibody	Catalogue number	Dilutions
DNMT1	#5032S (Cell Signalling Technology)	1:500
DNMT3a	#3598S (Cell Signalling Technology)	1:500
MBD2	sc-271562 (Santa Cruz)	1:500

3.6. ENZYME-LINKED IMMUNOSORBENT ASSAY (ELISA)

3.6.1. Introduction

ELISA relies on antigen-antibody interactions to quantify substances in a given sample (Figure 3.4) (Sakamoto et al., 2018). The specific antibody is attached to the solid surface of the plate, and the antigen in the sample binds to the antibody. The addition of a detection antibody results in the formation of an antigen-antibody complex (Sakamoto et al., 2018). The detection antibody is enzyme-conjugated, and the substrate added reacts with the enzyme to form a coloured product which is measured spectrophotometrically. The intensity of the colour produced is an indication of the concentration of the antigen in the given sample (Sakamoto et al., 2018).

3.6.2. Protocol

Control and treated cell supernatants were obtained and used for the quantification of DNMT3b using an ELISA kit (Thermo-Fisher Scientific, EH158RB). DNMT3b standards were prepared as per the manufacturer's protocol (0, 0.614, 1.536, 3.840, 9.600, 24, 60, and 150 ng/mL), and 100 µL of each standard and sample was added to predesignated wells. The plate was incubated (2.5 h, RT) on a shaker, following which the wells were washed four times with wash buffer (300 µL). Biotin conjugate (100 µL) was added, and the plate was incubated again (1 h, RT) on a shaker. Following incubation, the wells were washed four times with 300 µL of wash buffer. Streptavidin-HRP (100 µL) was added to each well and the plate was incubated (45 min, RT) with gentle shaking, following which the wells were washed as per the previous steps. TMB Substrate (100 µL) was added, and the plate was incubated (30 min, RT) in the dark on a shaker. A blue colour change was observed. Finally, stop solution (50 µL) was added and the colour changed to yellow. Absorbances were read spectrophotometrically at 450 nm using a microplate reader (BioTek µQuant Plate Reader). A standard curve was constructed, and sample DNMT3b concentrations were extrapolated.

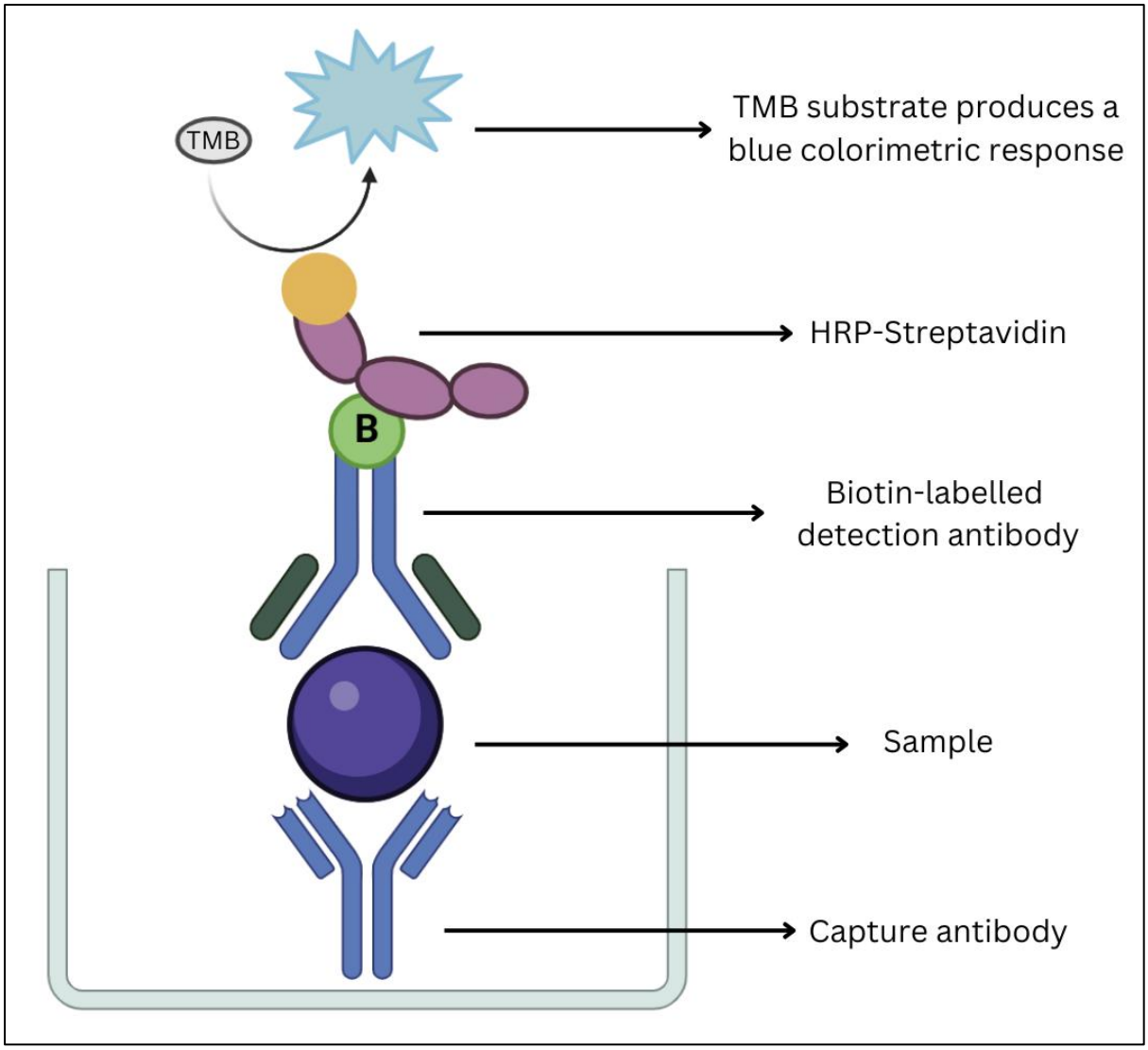

Figure 3.4: Overview of the ELISA procedure (prepared by author).

3.7. RNA ISOLATION

3.7.1. Introduction

RNA is extracted from cells using Qiazol reagent, which disrupts cell membranes without damaging RNA (El-Ashram et al., 2016). Once chloroform is added, phase separation occurs, by which protein remains at the lower organic phase, DNA is at the interface, and RNA is at the higher aqueous phase (Chomczynski and Sacchi, 2006). The addition of isopropanol to the extracted aqueous phase precipitates the RNA, and ethanol washes the RNA pellet. Finally, the resuspension of RNA occurs in nuclease-free water because it protects the RNA from degradation (El-Ashram et al., 2016).

3.7.2. Protocol

Control and treated Caco-2 cells were bathed in 0.1 M PBS thrice, then incubated with Qiazol and 0.1 M PBS (500 µL each, 5 min, RT). The cells were mechanically lysed by scraping, and homogenates were carefully decanted into 1.5 mL micro-centrifuge tubes and stored overnight at -80°C. The following day, chloroform (100 µL) was added to the thawed samples, and the tubes were centrifuged (12 000 x g, 15 min, 4°C). The RNA-containing aqueous phase was transferred into new 1.5 mL micro-centrifuge tubes on ice. Isopropanol (250 µL) was added, and the samples were stored overnight at -80°C. The following day, after thawing on ice, the samples were centrifuged again (12 000 x g, 20 min, 4°C). The supernatant was removed, and the pellet was washed with cold ethanol (75%, 500 µL), followed by centrifugation (7 400 x g, 15 min, 4°C). The ethanol was removed, and the RNA pellets were air-dried (30 min, RT). The dried pellets were then resuspended in 15 µL nuclease-free water and stored at -80°C.

The Nanodrop 2000 spectrophotometer (Thermo-Fisher Scientific, Waltham, USA) was used to quantify the isolated RNA, which was then standardised to the lowest concentration (200 ng/µL) with nuclease-free water. RNA purity was assessed using the A260/A280 absorbance ratio; a ratio between ~1.91 to 2.10 was considered pure (Ghazi et al., 2022).

3.8. QUANTITATIVE POLYMERASE CHAIN REACTION

3.8.1. Introduction

Quantitative PCR (qPCR) is a cyclic technique used to amplify and quantify DNA (Figure 3.5) (Garibyan and Avashia, 2013). Before performing qPCR, isolated RNA is reverse transcribed to produce complementary DNA (cDNA) which acts as a template for the amplification process. qPCR involves three main steps, repeated for 30 to 40 cycles:

1. Denaturation: The double-stranded DNA is heated to 95-96°C, causing separation of the strands into single-stranded DNA.
2. Annealing: The primers bind to their complementary target DNA sequences at a temperature specific to each primer.
3. Extension: DNA polymerase synthesises new DNA strands by adding nucleotides at 72°C.

The steps are repeated cyclically, resulting in exponential amplification of the target DNA sequence (Garibyan and Avashia, 2013). SYBR Green is used for the detection of the quantity of the target genes expressed by binding to the qPCR product DNA, emitting a fluorescent signal that is quantified.

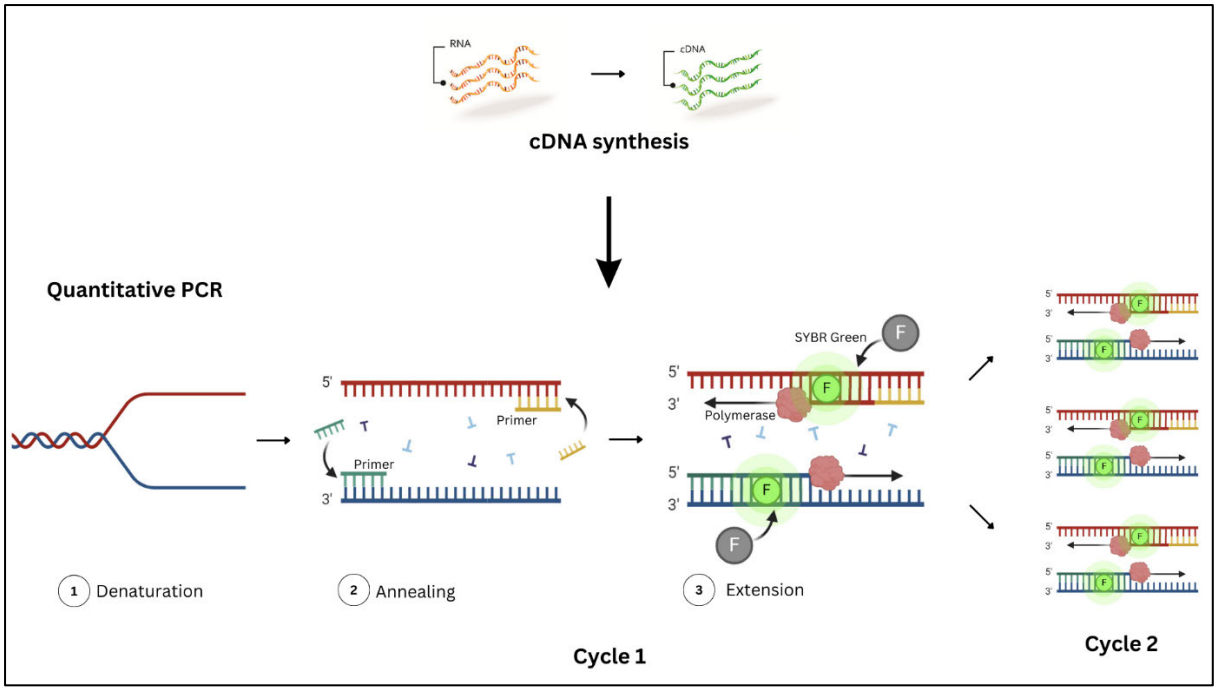

Figure 3.5: Overview of qPCR (prepared by author).

3.8.2. Protocol

3.8.2.1. cDNA synthesis

cDNA was synthesised from standardised RNA using the Maxima™ H Minus First Strand cDNA synthesis kit (Thermo-Fisher Scientific, K1652) (Table 2). The thermocycler settings were as follows:

- 10 min at 25°C
- 15 min at 50°C
- 5 min at 85°C

The cDNA was then suspended in nuclease-free water (60 µL) and stored at -80°C for subsequent qPCR assays.

Table 2: cDNA synthesis mix (Maxima™ H Minus First Strand cDNA synthesis kit)

Component	**One reaction volume (µL)**
10 mM dNTP mix	1
Oligo (dT) primer	0.25
Nuclease-free water	8.75
5 x RT buffer	4
Maxima H minus enzyme mix	1

Template DNA	5
TOTAL	**20 µL**

3.8.2.2. Determination of mRNA expression

Gene expression of *DNMT1, DNMT3a, DNMT3b, MBD2, UHRF1, TET1, TET2, TET3,* and *miR-29b* was assessed using the PowerUp™ SYBR™ Green Master mix (Thermo-Fisher Scientific). The reaction volumes were prepared according to the specifications in Table 3, and the forward and reverse primer sequences are provided in Table 4.

Sample amplification was performed using the QuantStudio™ 3 Real-Time PCR System (Thermo-Fisher Scientific), with the cycling conditions set as follows:

- Initial denaturation: 8 minutes at 95°C
- 40 cycles of:
  - Denaturation: 15 seconds at 95°C
  - Annealing: 40 seconds at a temperature specific to the gene of interest (Table 4)
  - Extension: 30 seconds at 72°C

Glyceraldehyde-3-phosphate dehydrogenase (GAPDH) was used as a housekeeping gene for normalising gene expression.

Table 3: qPCR reaction mix

Component	**One reaction volume (µL)**
PowerUp™ SYBR™ Green Master mix	5
RNAse-free water	1
Sense primer (25 µM)	1
Anti-sense primer (25 µM)	1
cDNA	2
TOTAL	**10 µL**

Table 4: The primer sequences and annealing temperatures used in qPCR

Primer	Sequence	Annealing temperature (°C)
DNMT1	Sense: ACCGCTTCTACTTCCTCGAGGCCTA Anti-sense: GTTGCAGTCCTCTGTGAACACTGTGG	58
DNMT3a	Sense: 5'-GCCAAAACTGCAAGAACTGCTTT-3' Anti-sense: 5'-CAGGAGGCGGTAGAACTCAAAGA-3'	62
DNMT3b	Sense: 5'-CCTTCCTGGGTCTACCACTCAGA-3' Anti-sense: 5'-GCTCCTTGCTTCACACTCCTCTC-3'	58
MBD2	Sense: 5'-AAACAGAGACTGCGAAACGATCC-3' Anti-sense: 5'-TGCAGAGGGGTTGAGATGTGTTA-3'	56
UHRF1	Sense: 5'-GCCATACCCTCTTCGACTACG-3' Anti-sense: 5'-GCCCCAATTCCGTCTCATCC-3'	58
TET1	Sense: CATCAGTCAAGACTTTAAGCCCT Anti-sense: CGGGTGGTTTAGGTTCTGTTT	62
TET2	Sense: GATAGAACCAACCATGTTGAGGG Anti-sense: TGGAGCTTTGTAGCCAGAGGT	62
TET3	Sense: TCCAGCAACTCCTAGAACTGAG Anti-sense: AGGCCGCTTGAATACTGACTG	56
miR-29b	Sense: 5'-GCGCGCTAGCACCATTTG-3' Anti-sense: 5'-CAGTGCAGGGTCCGAGGT-3'	62

The comparative threshold cycle (C_t) method (Livak and Schmittgen, 2001) was used to determine relative changes in mRNA expression: the fold change in expression relative to the control was calculated with the formula $2^{-\Delta\Delta Ct}$.

3.9. DNA ISOLATION

3.9.1. Introduction

DNA is extracted from cells using several reagents (El-Ashram et al., 2016). Lysis buffer is added first for the disruption of cell membranes. It contains Tris-Cl, SDS, and EDTA, all of which serve specific functions to ensure efficient DNA extraction. Tris-Cl is responsible for pH control during the extraction process. SDS lyses cell membranes to expose DNA. EDTA acts as a chelating agent and prevents the degradation of DNA. The addition of acetate salts serves to clump RNA, proteins, and lipids together for easy removal by centrifugation. Isopropanol precipitates DNA out of the solution, and ethanol is used to wash the resultant DNA pellet. Finally, TE buffer (also called DNA hydration solution) resolubilises the DNA sample for quantification and further use.

3.9.2. Protocol

Control and treated Caco-2 cells were bathed in 0.1 M PBS thrice, then incubated in cell lysis buffer (600 µL, 15 min, RT). Following incubation, the cells were mechanically lysed by scraping, and potassium acetate buffer (600 µL) was added. The sample was then invert mixed for 8 min, followed by vortexing and centrifugation (13 000 rpm, 5 min, RT). The DNA-containing supernatant was carefully decanted into 1.5 mL micro-centrifuge tubes, following which 100% isopropanol (600 µL) was added. The solution was invert mixed (5 min) and centrifuged (13 000 rpm, 5 min, RT). The isopropanol was discarded, and 100% ethanol (300 µL) was added to wash the pellet. After vortexing, the sample was centrifuged again (13 000 rpm, 5 min, RT). The ethanol was carefully removed, and the DNA pellet was allowed to air dry (15 min, RT). Once dry, the DNA pellets were resuspended in 10X TE buffer (40 µL), heated in a 65°C water-bath for 15 min, and then allowed to cool at RT.

The Nanodrop 2000 spectrophotometer (Thermo-Fisher Scientific, Waltham, USA) was used to quantify the isolated DNA, which was subsequently standardised to the lowest concentration (100 ng/µL) with 10X TE buffer. DNA purity was determined using the A260/A280 absorbance ratio; a ratio of ~1.70 to 1.90 was considered pure.

3.10. QUANTIFICATION OF GLOBAL DNA METHYLATION

3.10.1. Introduction

Global DNA methylation is evaluated by calculating the percentage of 5-methylcytosine (5mC) content in a DNA sample (Figure 3.6) (Couldrey and Cave, 2014). Following DNA isolation, the DNA samples are fixed to strip wells with a high affinity for DNA. The 5mC content was

determined using capture and enzyme-conjugated detection antibodies. Enhancer and developer solutions react with the detection antibody to produce a colorimetric response which is quantified spectrophotometrically. The intensity of the colour produced is a direct indication of the 5mC content in the sample.

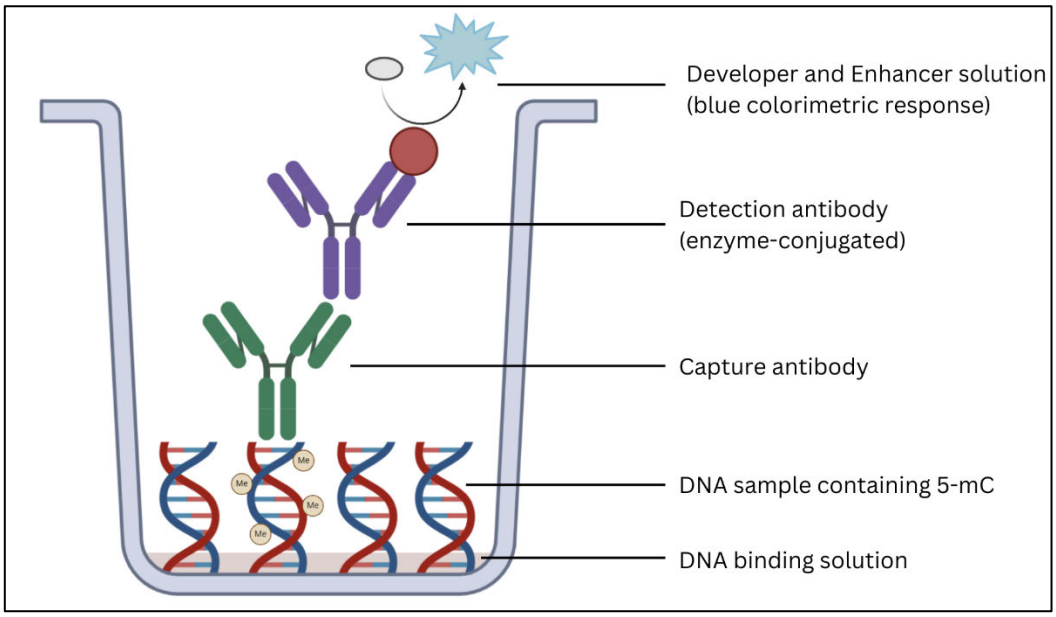

Figure 3.6: Principle of the quantification of DNA methylation (prepared by author).

3.10.2. Protocol

Isolated DNA was used for the quantification of global methylation using the Colorimetric Methylated DNA Quantification Kit (Abcam, ab117128). Positive controls were prepared (0-10 ng/µL) with 1 X TE buffer. Binding solution (80 µL) was added to each well. Negative controls (1 µL), positive controls (1 µL), and 100 ng of sample DNA were added to their predesignated wells. The solutions were gently mixed to ensure even coating of the bottom of the wells. The plates were covered with a plate seal and incubated (90 min, 37°C) to allow DNA binding.

Following incubation, the binding solution was removed, and the wells were washed thrice with 1 X wash buffer (150 µL). Capture antibody (1:1 000; 50 µL) was added, and the plate was covered and incubated (60 min, RT). The capture antibody was removed, and each well was washed thrice with wash buffer (150 µL). Detection antibody (1:2 000; 50 µL) was added, and the plate was covered and incubated (30 min, RT). Detection antibody was removed, and each well was washed four times with wash buffer (150 µL). Enhancer solution (1:5 000; 50

μL) was added, and the plate was covered and incubated (30 min, RT). Enhancer solution was removed, and the wells were washed five times with wash buffer (150 μL).

Developer solution (100 μL) was added, and the plate was incubated in the dark (10 min, RT) while colour change was monitored. Stop solution (50 μL) was added and the colour changed to yellow. Absorbances were measured at 450 nm using a microplate reader (BioTek μQuant Plate Reader).

A standard curve with the positive controls was constructed as per manufacturer's guidelines. The 5mC content was calculated using the following equations:

$$5\text{mC (ng)} = \frac{\text{Sample OD} - \text{Negative Control OD}}{\text{Slope} \times 2}$$

$$5\text{mC \%} = \frac{5\text{mC (ng)}}{\text{Input DNA (ng)}} \times 100$$

The results were represented as fold-change relative to the control.

3.11. STATISTICAL ANALYSIS

Data analysis was conducted using GraphPad Prism v5.0 (GraphPad Prism Software Inc.). Statistical significance was determined by one-way analysis of variance (ANOVA) with Bonferroni multiple comparisons test. Results were expressed as mean fold-change ± standard deviation (SD). All experiments were carried out three times in triplicate, unless otherwise stated. *P*-values below 0.05 were considered significant.

3.12. ETHICS APPROVAL

This study was granted ethics approval by BREC (reference number: BREC/00006233/2023).

CHAPTER 4: RESULTS

TQ decreased Caco-2 cell viability

The MTT assay was used to determine the effect of TQ on Caco-2 cell viability. Cells were treated with a range of concentrations of TQ (0-800 μM) for 24 hours. A dose-dependent decrease in cell viability was evident, with higher TQ concentrations resulting in greater cytotoxicity (Figure 4.1). A concentration of 504.2 μM TQ was calculated at 50% cell viability (IC_{50}); this concentration was used for subsequent assays.

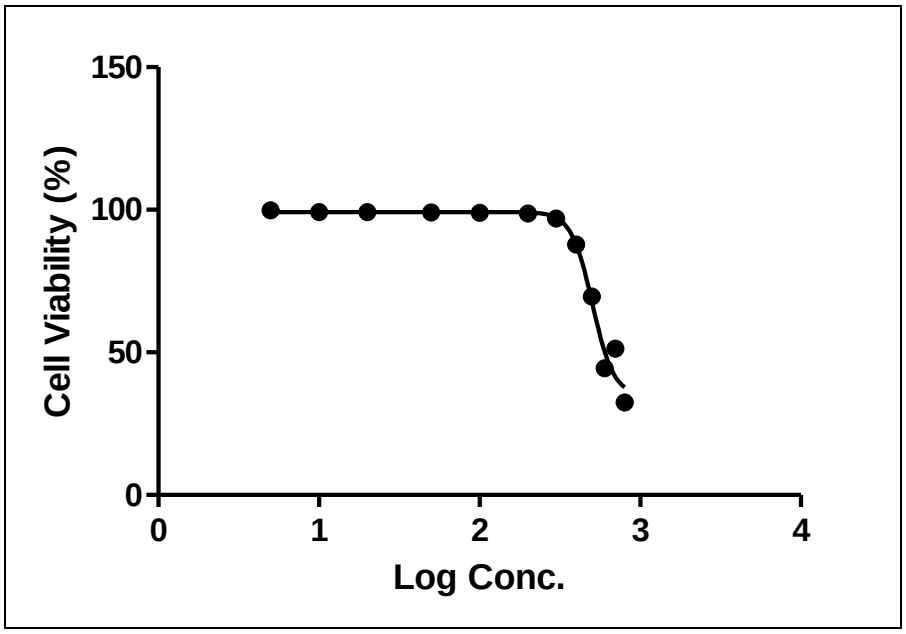

Figure 4.1: TQ was toxic to Caco-2 cells. TQ caused a dose-dependent decrease in Caco-2 cell viability. An IC_{50} of 504.2 μM was calculated.

TQ induced global DNA hypomethylation in Caco-2 cells

The effect of TQ on global DNA methylation was evaluated by measuring the percentage of 5mC using a colorimetric kit. The results indicated a significant reduction in 5mC levels in TQ-treated cells when compared to the control group ($p = 0.0008$, Figure 4.2), indicating that TQ caused global DNA hypomethylation in Caco-2 cells.

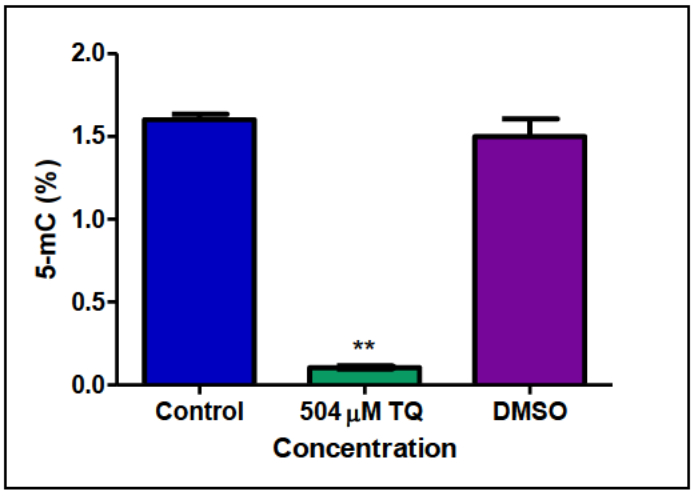

Figure 4.2: TQ induced global DNA hypomethylation in Caco-2 cells. TQ decreased the percentage of 5mC in TQ-treated cells compared to the control (**$p < 0.005$).

TQ reduced DNMT1, DNMT3a, and DNMT3b expression in Caco-2 cells

The DNMT family plays a vital role in the initiation and maintenance of DNA methylation. We assessed the effect of TQ on *DNMT1*, *DNMT3a*, and *DNMT3b* mRNA expression through qPCR. TQ treatment significantly reduced the mRNA expression of *DNMT1* ($p = 0.0280$, Figure 4.3), *DNMT3a* ($p = 0.0130$, Figure 4.3), and *DNMT3b* ($p = 0.0028$, Figure 4.3) in Caco-2 cells compared to the control. Western blotting or ELISA confirmed that TQ also significantly decreased protein expression of DNMT1 ($p < 0.0001$, Figure 4.4A), DNMT3a ($p < 0.0001$, Figure 4.4B), and DNMT3b ($p = 0.0064$, Figure 4.4C) compared to the control.

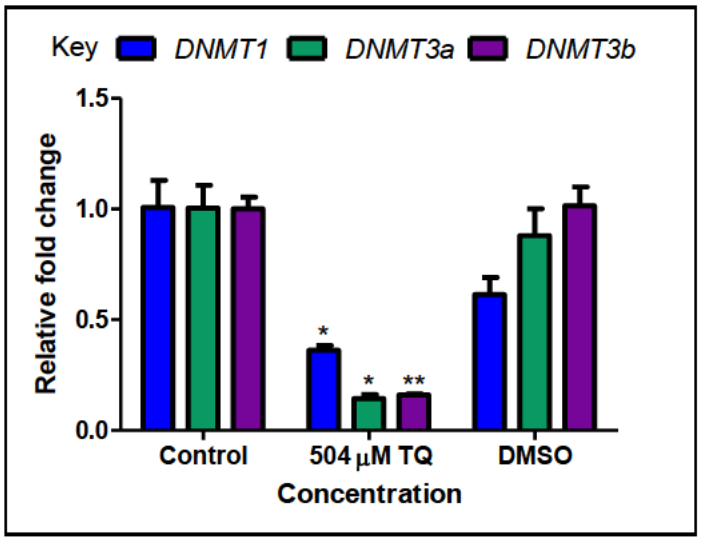

Figure 4.3: The effect of TQ on mRNA expression of DNMTs in Caco-2 cells. TQ significantly decreased mRNA expression of *DNMT1, DNMT3a,* and *DNMT3b* in Caco-2 cells compared to the control (*$p < 0.05$, **$p < 0.005$).

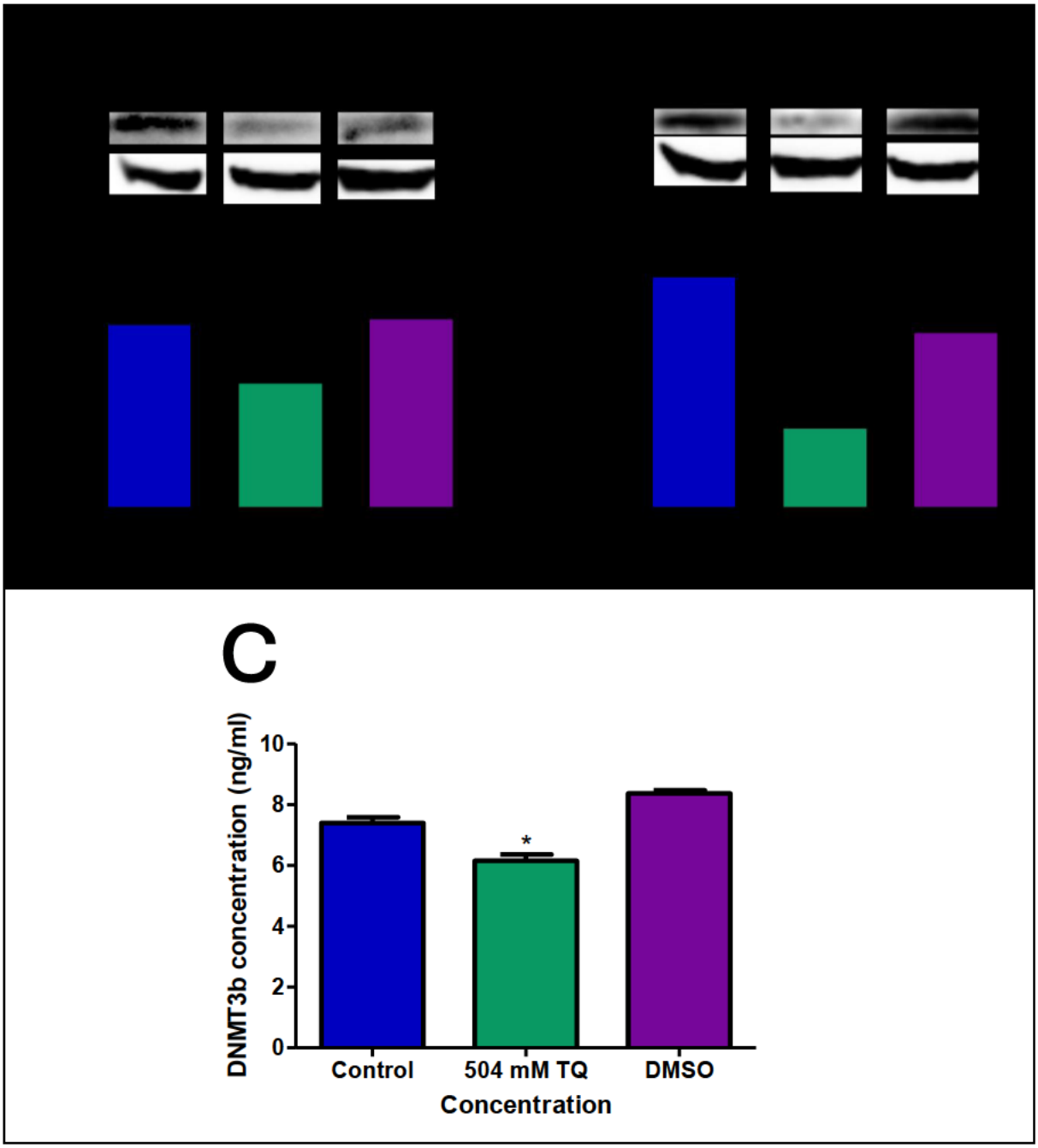

Figure 4.4: The effect of TQ on protein expression of DNMT1, DNMT3a, and DNMT3b in Caco-2 cells. Protein expression of DNMT1 **(A)**, DNMT3a **(B)**, and DNMT3b **(C)** were significantly downregulated in TQ-treated Caco-2 cells compared to the control (*$p < 0.05$, ***$p < 0.0001$).

TQ increased *miR-29b* expression in Caco-2 cells

MiR-29b is known to negatively regulate the expression of all three DNMTs; therefore, we assessed whether the decrease in *DNMT* expression could be as a result of miR-29b. qPCR analysis revealed that TQ significantly increased the expression of *miR-29b* ($p = 0.0149$, Figure 4.5) in Caco-2 cells compared to the control. These findings imply that the observed reduction in *DNMT* expression and resultant global DNA hypomethylation may be facilitated by the upregulation of miR-29b.

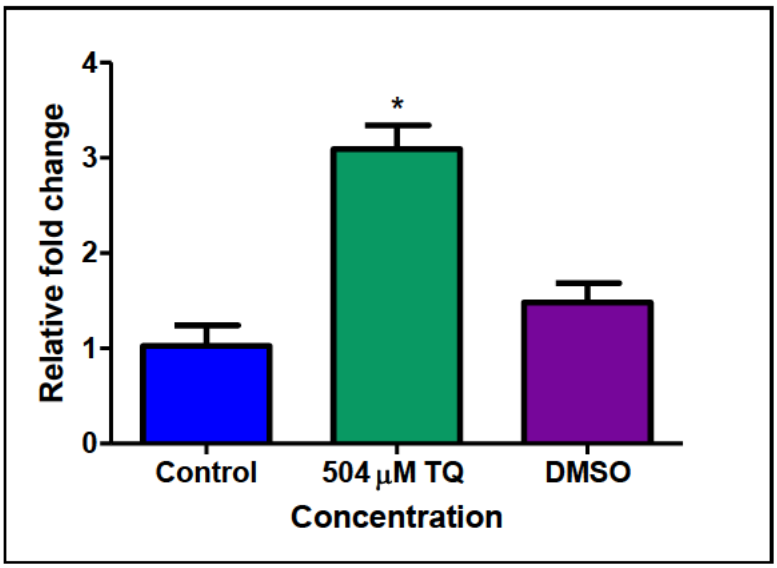

Figure 4.5: The effect of TQ on miR-29b expression in Caco-2 cells. MiR-29b expression was significantly upregulated in TQ-treated Caco-2 cells compared to the control (*$p < 0.05$).

TQ decreased *UHRF1* expression in Caco-2 cells

UHRF1 acts as a cofactor to DNMT1 by binding to hemimethylated DNA and recruiting DNMT1 for the maintenance of methylation. We determined if the global DNA hypomethylation observed could be attributed to decreased DNMT1 activity through decreased UHRF1 expression. qPCR analysis revealed that TQ significantly decreased *UHRF1* mRNA expression ($p = 0.0378$, Figure 4.6) in Caco-2 cells compared to the control. This indicated that

DNMT1 activity was reduced, which contributed to the global DNA hypomethylation observed in TQ-treated Caco-2 cells.

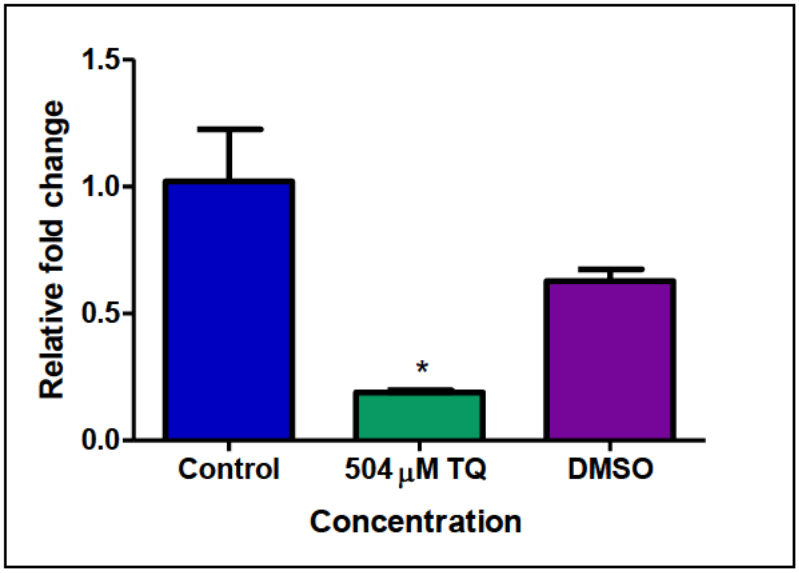

Figure 4.6: The effect of TQ on mRNA expression of *UHRF1* in Caco-2 cells. TQ significantly decreased gene expression of *UHRF1* in Caco-2 cells compared to the control (*$p < 0.05$).

TQ decreased expression of MBD2 in Caco-2 cells

MBD2 is associated with DNA methylation-mediated gene silencing by binding to 5mC of hypermethylated DNA and facilitating transcriptional repression. We assessed the contribution of MBD2 to the observed DNA hypomethylation and transcriptional silencing by examining both its gene and protein expression. qPCR and Western blot analyses revealed a significant decrease in MBD2 expression at both the mRNA ($p = 0.0097$, Figure 4.7A) and protein levels ($p = 0.0011$, Figure 4.7B) in Caco-2 cells as compared to the control. These results indicated that the TQ-induced decrease in MBD2 expression is linked to the reduction in DNA methylation.

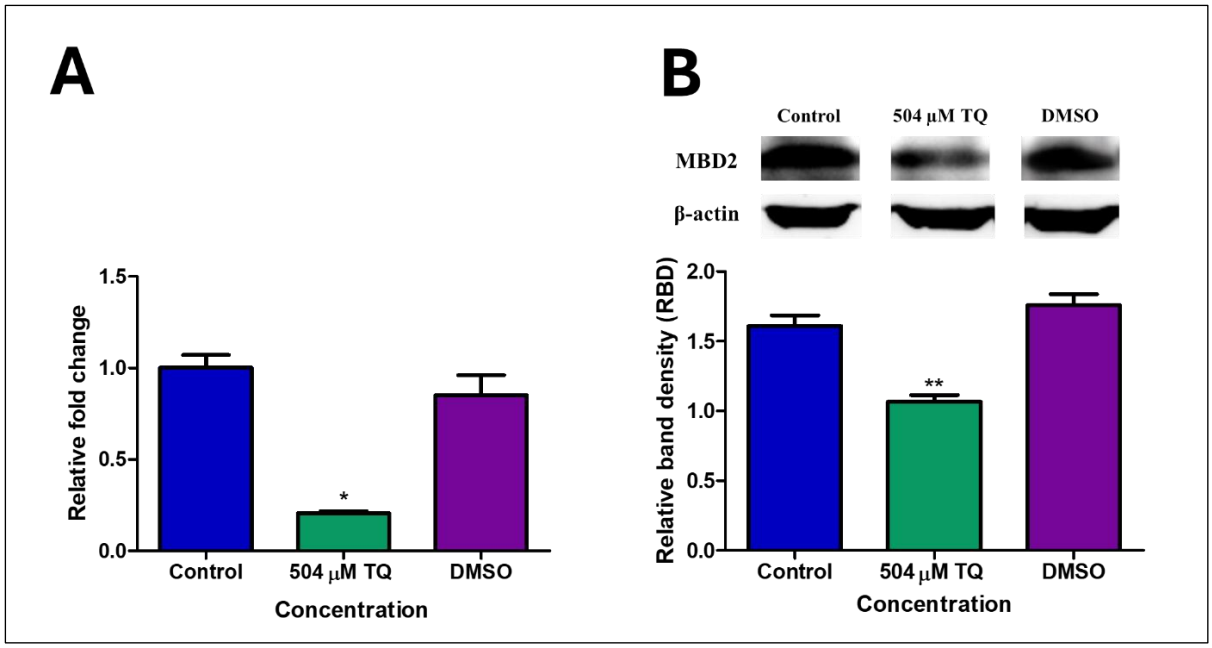

Figure 4.7: The effect of TQ on MBD2 expression in Caco-2 cells. **(A)** TQ significantly decreased mRNA expression of *MBD2* in Caco-2 cells compared to the control. **(B)** TQ significantly decreased protein expression of MBD2 in Caco-2 cells compared to the control (*$p < 0.05$, **$p < 0.005$).

TQ increased DNA demethylation in Caco-2 cells through increased *TET1-3* expression

DNA methylation is reversed by TET proteins, which convert 5mC back to cytosine. We determined if the global DNA hypomethylation observed in TQ-treated cells occurred due to TET1-3 through qPCR analysis of their mRNA expression. TQ significantly upregulated the expression of *TET1* ($p = 0.0124$, Figure 4.7), *TET2* ($p = 0.0109$, Figure 4.8), and *TET3* ($p = 0.0004$, Figure 4.7) in Caco-2 cells compared to the control. This indicated that DNA demethylation occurred in TQ-treated cells.

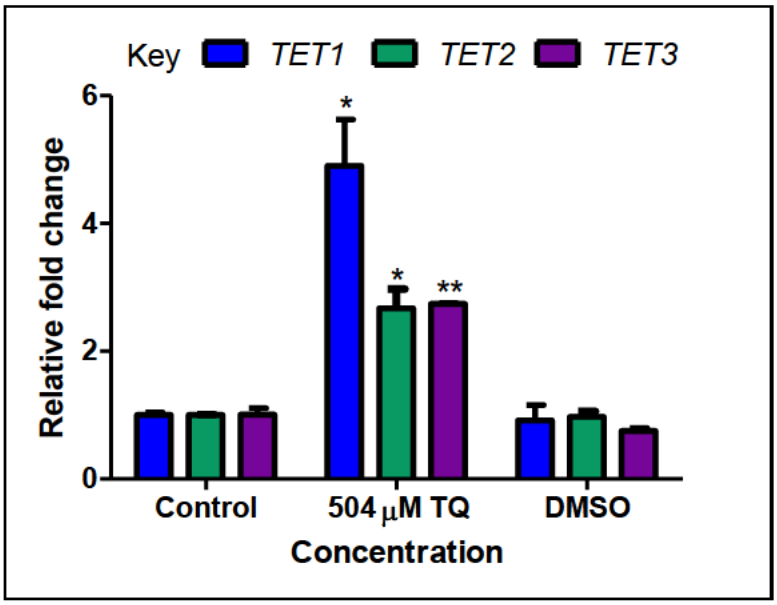

Figure 4.8: TQ significantly upregulated the mRNA expression of *TET1, TET2,* and *TET3* in Caco-2 cells compared to the control (*$p < 0.05$, **$p < 0.005$).

CHAPTER 5: DISCUSSION

TQ, found in the herb *Nigella sativa*, is known to produce a variety of therapeutic responses to several diseases, the most prominent being anticancer effects. Several different anticancer mechanisms of TQ have been described, including its effects on epigenetic mechanisms (Khan et al., 2019); however, its role in affecting epigenetics in colorectal cancer is still unclear. DNA methylation is a significant epigenetic alteration that affects gene expression, and abnormal hypermethylation patterns have been observed in various cancers, including colorectal cancer. In fact, aberrant methylation patterns in general are reported to predispose to a cancer phenotype (Chen et al., 2022). This study aimed to assess the influence of TQ on global DNA methylation in Caco-2 cells, and the results support the hypothesis that TQ triggers global DNA hypomethylation in colorectal adenocarcinoma cells, contributing to cell death.

The MTT assay was conducted to evaluate the effect of TQ on Caco-2 cell viability. A dose-dependent reduction in cell viability was observed (Figure 4.1), suggesting that TQ is highly toxic to the Caco-2 cell line at increasing concentrations. This is consistent with findings from several other studies where TQ was shown to be toxic to cancer cells (Aslan et al., 2021, Dera and Rajagopalan, 2019, Kus et al., 2018). A study by Ramzy et al. (2020) indicated IC_{50} concentrations of 58 µM and 38 µM after exposure of Caco-2 cells to TQ for 24 hours and 48 hours, respectively. This differs from the IC_{50} value obtained in this study (504 µM). The discrepancy may be due to differences in the concentration ranges used: Ramzy et al. (2020) employed a narrower range (0-400 µM), while the present study used a broader range (0-800 µM). Additionally, the deviation in IC_{50} values may be attributed to differences in cell seeding density. While Ramzy et al. (2020) seeded 2 000-10 000 cells/well, the present study used a density of 15 000 cells/well. Furthermore, differences in the MTT assay protocols used may also explain the variation. Following treatment with TQ, Ramzy et al. (2020) incubated the cells with MTT salt for 2 hrs and the purple formazan crystals were solubilized for 30 min. In contrast, cells were incubated with MTT salt for 4 hrs and the purple formazan crystals were solubilized for 1 hr in the present study. Being a colorimetric assay, these longer incubation periods in combination with the high cell seeding density could have intensified the purple colour produced yielding a higher IC_{50}. This is consistent with findings by Ghasemi et al. (2021), which showed that higher cell seeding densities and longer incubation periods increased the optical density measured. Thus, the results of the present study provide insight into the cytotoxic mechanisms of TQ at an epigenetic level.

DNA methylation is primarily controlled by the DNA methyltransferases DNMT1, DNMT3a, and DNMT3b. The former is responsible for maintaining established methylation patterns, while the latter two ensure *de novo* methylation. These methyltransferases are often evidenced to be upregulated in cancers, including colorectal cancer, and silencing their expression has been shown to restore expression of TSGs and promote cell death (Subramaniam et al., 2014). In this study, TQ triggered global DNA hypomethylation in Caco-2 cells, as demonstrated by a significant reduction in the percentage of 5-methylcytosine (Figure 4.2). This hypomethylation is associated with downregulated mRNA expression of *DNMT1, DNMT3a,* and *DNMT3b* (Figure 4.3) as well as decreased protein expression (Figure 4.4). These findings agree with previous studies in which TQ reduced the expression of DNMTs (Al-Rawashde et al., 2021, Qadi et al., 2019). Based on these observations, it is likely that the TQ-induced decrease in DNA methylation observed in this study leads to the re-expression of TSGs to promote cell death and describes a potential mechanism for the cytotoxicity displayed.

MicroRNAs are responsible for the post-transcriptional negative regulation of gene expression by targeting specific mRNA for degradation or preventing its translation. MiR-29b is known to regulate *DNMT3a* and *DNMT3b* directly, and *DNMT1* indirectly through its transcription factor *Sp1* (Garzon et al., 2009). As such, this regulation results in the inhibition of DNA methylation. Interestingly, miR-29b expression is often downregulated in several types of cancers, which correlates with an increase in *DNMT* expression (Jiang et al., 2014). The present study indicated that TQ significantly upregulated miR-29b expression in Caco-2 cells (Figure 4.5), which was inversely related to *DNMT1, DNMT3a*, and *DNMT3b* expression as well the global DNA methylation status. This suggests that the TQ-induced upregulation of miR-29b expression may play a significant role in the evident global DNA hypomethylation, as high miR-29b expression will result in the degradation of *DNMT* transcripts. Other studies have exhibited that TQ upregulates miR-29b expression in leukaemia cells and disrupts the Sp1/Nfκ-B complex, leading to the inhibition of *DNMT1* expression (Pang et al., 2017). Additionally, enforced miR-29b expression in other cancer cell lines, namely lung cancer and lymphoma, has been shown to decrease *DNMT3a* and *DNMT3b* expression, thereby, inducing DNA hypomethylation (Fabbri et al., 2007, Mazzoccoli et al., 2018). Therefore, the results of the present study support these findings that the TQ-induced upregulation of miR-29b expression provides an alternative mechanism for the reduction in DNMT expression and subsequent global DNA hypomethylation. No literature is available regarding the direct mechanisms of TQ-induced miR-29b activation, as the present study provides a fairly novel perspective on the

influence of TQ on miR-29b expression. Interestingly, however, based on the study conducted by Pang et al. (2017) that reported an increase in miR-29b expression following exposure to TQ, it can be postulated that Sp1 expression was downregulated, noting the known role of miR-29b in DNA methylation. Reduced Sp1 levels may potentially contribute to the cytotoxicity observed in this study, as it is involved in cell cycle progression (Vellingiri et al., 2020): downregulation of Sp1 could lead to cell cycle arrest and apoptosis. Hence, this further supports the idea that upregulated miR-29b expression may play a role in the observed cytotoxic effects.

UHRF1, an E3 ubiquitin ligase, functions as a cofactor for DNMT1 and is critical for maintaining DNA methylation. UHRF1 binds to hemimethylated DNA by means of its SRA domain, recruiting DNMT1 to propagate DNA methylation patterns. Overexpression of UHRF1 has been linked to DNA hypermethylation in several cancers, including colorectal cancer, due to its role in ensuring DNMT1 activity (Ashraf et al., 2017, Kong et al., 2019). *UHRF1* expression in TQ-treated Caco-2 cells was significantly downregulated in this study (Figure 4.6), suggesting a concomitant decrease in DNMT1 activity. This likely contributed to the observed DNA hypomethylation, as the reduced presence of UHRF1 would impair the ability of DNMT1 to maintain DNA methylation. These results correspond with previous studies in which TQ decreased UHRF1 expression and DNMT1 activity, leading to the upregulation of TSGs (Abusnina et al., 2011, Alhosin et al., 2020, Ibrahim et al., 2018). In fact, knockdown of UHRF1 expression in several cancer cell lines has been shown to reduce DNA methylation, reactivate TSG expression, and induce apoptosis (Nishiyama and Nakanishi, 2021). Thus, the decrease in *UHRF1* expression observed in this study likely provides another alternative mechanism for the reduction in global DNA methylation in TQ-treated Caco-2 cells. Interestingly, a study by Liu et al. (2024) demonstrated that UHRF1 knockdown in breast cancer cells caused cell cycle arrest as well as apoptosis. Therefore, the TQ-induced downregulation of *UHRF1* evident in this study may play a role in inducing cell death through both cell cycle arrest and apoptosis. This suggests that the cytotoxicity evident here may occur not only through the re-expression of previously methylated TSGs, but also through the downregulation of UHRF1. Hence, the impact of UHRF1 downregulation may be two-fold: decreased DNMT1 activity to contribute to DNA hypomethylation, and cytotoxicity by inducing cell cycle arrest and apoptosis.

In addition to altering DNA methylation through DNMT and UHRF1 expression, TQ may also influence gene silencing by modulating the expression of the methyl-CpG-binding domain 2 (MBD2) protein. MBD2 expression is methylation-dependent as it binds to 5mC to prevent

binding of transcription factors and promote transcriptional silencing (Wood and Zhou, 2016). MBD2 is often overexpressed in cancers, including colorectal cancer, where it contributes to silencing of TSGs; this correlates with the hypermethylation state (Wood and Zhou, 2016). In this study, TQ significantly reduced both mRNA and protein expression of MBD2 (Figure 4.7), suggesting that decreased MBD2 expression contributes to TSG silencing. This is associated with the global DNA hypomethylation observed. Since MBD2 expression is methylation-dependent, decreased DNA methylation (and decreased 5mC content) induces downregulation of MBD2 expression. In fact, poorly methylated regions of DNA contain lower levels of MBD2 (Wood and Zhou, 2016). In this way, decreased MBD2 expression is associated with the re-expression of TSGs. This corresponds with previous studies, in which knockdown of MBD2 expression in colon, prostate, and brain cancer cell lines was related to restoration of TSG expression through DNA hypomethylation (Martin et al., 2008, Stirzaker et al., 2017, Zhu et al., 2011). It should be noted, however, that MBD2-mediated transcriptional silencing occurs downstream of DNA methylation, and loss of MBD2 does not directly affect DNA methylation patterns; it merely facilitates the silencing of already methylated genes (Wang et al., 2024b). Thus, loss of MBD2 may serve as an indicator for reduced levels of methylation. Therefore, the TQ-induced decrease in MBD2 expression observed in the present study is likely associated with reactivation of TSG expression, via a decrease in its transcriptional silencing properties, and reduced global DNA methylation.

Two pathways that might influence expression of MBD2 are the Wnt pathway and the ERK1/2 pathway. The Wnt pathway is involved in intestinal homeostasis and stem cell maintenance. Dysregulated Wnt signalling has been observed in intestinal cancer, and loss of MBD2 served to attenuate Wnt signalling in intestinal cancer mice models (Phesse et al., 2008). The ERK1/2 pathway is known to be dysregulated in cancer, thereby promoting cancer cell growth. Loss of MBD2 served to decrease ERK1/2 signalling, resulting in decreased cancer cell growth (Xie et al., 2021). Notably, TQ has been evidenced to influence both Wnt and ERK1/2 signalling in cancer cell lines (Alam et al., 2022, Moulana et al., 2024). Thus, MBD2-mediated transcriptional silencing may potentially occur in association with these signalling pathways, with altered Wnt and ERK1/2 signalling likely occurring in the present study.

Global DNA hypomethylation may also be attributed to DNA demethylation, catalysed by ten-eleven translocation (TET) proteins. TET1-3 convert 5mC back to cytosine. In fact, under-expression of all three TET proteins has been reported in several cancers, corresponding with DNA hypermethylation (Rasmussen and Helin, 2016). TQ significantly increased the mRNA

expression of *TET1, TET2,* and *TET3* in Caco-2 cells (Figure 4.8), suggesting that, in addition to the downregulation in DNMTs, demethylation may have contributed to the global DNA hypomethylation observed in this study. TQ has previously been reported to increase *TET2* mRNA expression in chronic myeloid leukaemia (CML) cells, causing DNA hypomethylation, restoration of TSG expression, and apoptosis (Al-Rawashde et al., 2023). Thus, the TQ-induced increase in *TET1-3* expression in Caco-2 cells suggests demethylation of TSGs occurred to bring about cell death. Currently, no literature directly addresses the mechanisms underlying TQ-induced TET inhibition, as this study provides a novel overview of this effect. However, a potential mechanism can be hypothesised. The Nf-κB pathway has been shown to repress the expression of all three TET proteins (Collignon et al., 2018, Kaplanek et al., 2023, Zhu et al., 2021). Since TQ has been demonstrated to reduce Nf-κB signalling, this could be linked to the observed upregulation of *TET1-3* in the present study. Thus, the upregulation of *TET1-3* expression induced by TQ in Caco-2 cells may contribute to DNA demethylation and the reactivation of TSGs, ultimately promoting cell death, and further investigation into the underlying mechanisms of this effect is warranted.

Hence, the results of this study demonstrate that TQ induces toxicity in Caco-2 cells through global DNA hypomethylation (Figure 5.1). This effect was mediated by the cumulative downregulation of DNA methyltransferases (DNMT1, DNMT3a, and DNMT3b), the DNA maintenance cofactor *UHRF1*, and the methylation reader MBD2, along with the upregulation of *miR-29b* and the DNA demethylases *TET1*, *TET2*, and *TET3*. These changes likely led to the reactivation of silenced TSGs to induce cell death. Thus, the results of this study contribute to the growing evidence for the potential of TQ as a promising anticancer candidate that targets DNA methylation.

As evidenced in literature, TQ has been shown to influence oxidative stress, apoptosis, and autophagy in various cancer cell lines by altering multiple signalling pathways (Hannan et al., 2021). These processes must be considered when reporting the methods of TQ-induced cytotoxicity, as they are likely contributing factors. In the context of this study, the TSGs proposed to be re-expressed due to DNA hypomethylation may play a role in modulating oxidative stress, apoptosis, and/or autophagy. This is particularly significant because oxidative stress is known to impact DNA methylation patterns, which suggests a potential feedback loop (Wu and Ni, 2015). Consequently, the precise mechanisms of cell death observed in this study remains unclear. However, based on similar studies, it can be postulated that apoptosis is the primary mode of cell death, as several studies have reported the upregulation of caspases

alongside DNA hypomethylation following exposure to TQ. Therefore, while the exact mechanism of cell death in this study remains to be fully explored, the interplay between DNA hypomethylation, oxidative stress, autophagy, and apoptosis provides a possible outline for TQ-induced cytotoxicity. Further research is needed to clarify the mechanisms at play.

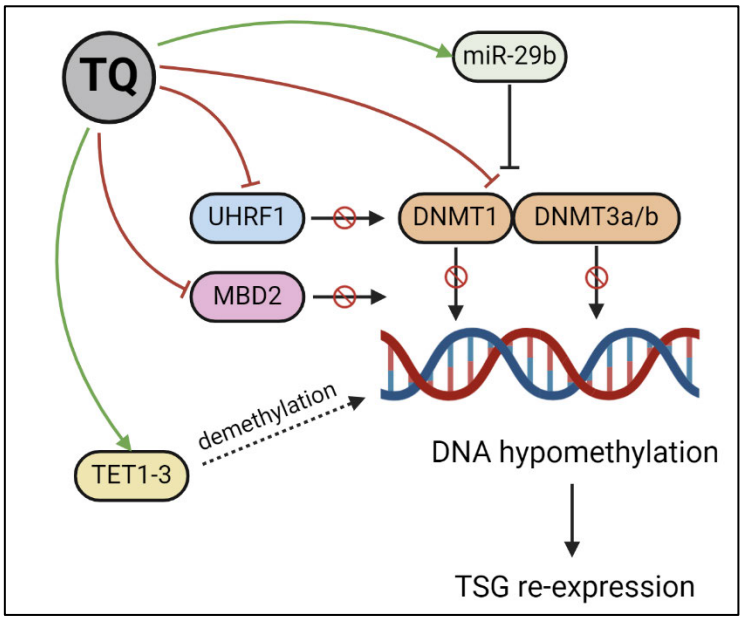

Figure 5.1: Proposed mechanism of the TQ-induced global DNA hypomethylation in Caco-2 cells. TQ downregulated the methyltransferases DNMT1, DNMT3a, and DNMT3b. UHRF1 expression was also downregulated, suggesting a concomitant decrease in DNMT1 activity and maintenance of methylation. Decreased expression of the methylation reader MBD2 served to attenuate methylation-dependent transcriptional repression. MiR-29b, known to negatively regulate the expression of DNMT1, DNMT3a, and DNMT3b, was upregulated, thereby contributing to decreased levels of the methyltransferases. The DNA demethylase proteins TET1, TET2, and TET3 were also upregulated to trigger demethylation. Altogether, these findings suggest that TQ induces global DNA hypomethylation through the mechanisms explained, likely leading to the reactivation of silenced TSGs to cause cell death.

CONCLUSION

In conclusion, this study provides valuable insight into the epigenetic mechanisms underlying TQ-induced cytotoxicity in human colorectal adenocarcinoma cells, further supporting its potential as an anticancer agent. Our findings demonstrate that TQ triggers global DNA hypomethylation by downregulating DNMT1, DNMT3a, DNMT3b, UHRF1, and MBD2 expression. Furthermore, the reduction in DNA methylation is linked to the upregulation of miR-29b, a miRNA known to target and suppress DNMT expression, which may be a key mechanism through which TQ mediates DNA hypomethylation. Additionally, the study reveals that TQ treatment increases the expression of the DNA demethylase proteins TET1, TET2, and TET3, which contribute to the reversal of DNA methylation, further promoting DNA hypomethylation. Altogether, these findings imply that the ability of TQ to modulate DNA methylation likely leads to the re-expression of TSGs that are silenced by DNA hypermethylation in cancer cells, ultimately leading to cell death. These results contribute to the growing evidence that the anticancer effects of TQ may be, in part, attributed to its effect on DNA methylation, which indicates that TQ could potentially become a promising anticancer candidate for further clinical investigation. This has especially significant implications in areas with limited access to conventional cancer therapies.

However, while TQ exhibits promising anticancer potential in *in vitro* studies, its poor bioavailability remains an obstacle. In fact, TQ has not yet been widely tested in anticancer clinical trials, likely due to challenges in delivery and absorption. To circumvent this, future studies could explore strategies to improve bioavailability, such as utilizing nanotechnology or modifying its chemical structure. Additionally, further methylation-specific studies involving gene sequencing to identify specific genes affected by TQ-induced changes in methylation would undoubtedly help better define its targets and prove to be fruitful in understanding the precise mechanisms displayed.

LIMITATIONS AND RECOMMENDATIONS

The present study investigated the epigenetic changes in Caco-2 cells resulting from exposure to TQ for a limited time of 24 hours. Only the IC_{50} concentration of TQ was used in treatments. The study was conducted using an *in vitro* model of colorectal cancer, and *in vivo* results may differ.

Hence, future studies should make use of an extended exposure protocol (such as 48 and 72 hours) with a range of treatment concentrations to allow for a broader perspective of the toxic effects of TQ. Additionally, studies using *in vivo* models of colorectal cancer would be useful to consolidate the results of the present study.

REFERENCES

ABUSNINA, A., ALHOSIN, M., KERAVIS, T., MULLER, C. D., FUHRMANN, G., BRONNER, C. & LUGNIER, C. 2011. Down-regulation of cyclic nucleotide phosphodiesterase PDE1A is the key event of p73 and UHRF1 deregulation in thymoquinone-induced acute lymphoblastic leukemia cell apoptosis. *Cell Signal,* 23**,** 152-60.

AHMAD, A., HUSAIN, A., MUJEEB, M., KHAN, S. A., NAJMI, A. K., SIDDIQUE, N. A., DAMANHOURI, Z. A. & ANWAR, F. 2013. A review on therapeutic potential of Nigella sativa: A miracle herb. *Asian Pac J Trop Biomed,* 3**,** 337-52.

AL-ALI, A., ALKHAWAJAH, A. A., RANDHAWA, M. A. & SHAIKH, N. A. 2008. Oral and intraperitoneal LD50 of thymoquinone, an active principle of Nigella sativa, in mice and rats. *J Ayub Med Coll Abbottabad,* 20**,** 25-7.

AL-RAWASHDE, F. A., AL-SANABRA, O. M., ALQARALEH, M., JARADAT, A. Q., AL-WAJEEH, A. S., JOHAN, M. F., WAN TAIB, W. R., ISMAIL, I. & AL-JAMAL, H. A. N. 2023. Thymoquinone Enhances Apoptosis of K562 Chronic Myeloid Leukemia Cells through Hypomethylation of SHP-1 and Inhibition of JAK/STAT Signaling Pathway. *Pharmaceuticals (Basel),* 16.

AL-RAWASHDE, F. A., JOHAN, M. F., TAIB, W. R. W., ISMAIL, I., JOHARI, S., ALMAJALI, B., AL-WAJEEH, A. S., NAZARI VISHKAEI, M. & AL-JAMAL, H. A. N. 2021. Thymoquinone Inhibits Growth of Acute Myeloid Leukemia Cells through Reversal SHP-1 and SOCS-3 Hypermethylation: In Vitro and In Silico Evaluation. *Pharmaceuticals (Basel),* 14.

ALAM, M., HASAN, G. M., ANSARI, M. M., SHARMA, R., YADAV, D. K. & HASSAN, M. I. 2022. Therapeutic implications and clinical manifestations of thymoquinone. *Phytochemistry,* 200**,** 113213.

ALHOSIN, M., OMRAN, Z., ZAMZAMI, M. A., AL-MALKI, A. L., CHOUDHRY, H., MOUSLI, M. & BRONNER, C. 2016. Signalling pathways in UHRF1-dependent regulation of tumor suppressor genes in cancer. *J Exp Clin Cancer Res,* 35**,** 174.

ALHOSIN, M., RAZVI, S. S. I., SHEIKH, R. A., KHAN, J. A., ZAMZAMI, M. A. & CHOUDHRY, H. 2020. Thymoquinone and Difluoromethylornithine (DFMO) Synergistically Induce Apoptosis of Human Acute T Lymphoblastic Leukemia Jurkat Cells Through the Modulation of Epigenetic Pathways. *Technol Cancer Res Treat,* 19**,** 1533033820947489.

ALI SYEDA, Z., LANGDEN, S. S. S., MUNKHZUL, C., LEE, M. & SONG, S. J. 2020. Regulatory Mechanism of MicroRNA Expression in Cancer. *Int J Mol Sci,* 21.

ALKHARFY, K. M., AHMAD, A., KHAN, R. M. & AL-SHAGHA, W. M. 2015. Pharmacokinetic plasma behaviors of intravenous and oral bioavailability of thymoquinone in a rabbit model. *Eur J Drug Metab Pharmacokinet,* 40**,** 319-23.

ANGELIS, I. D. & TURCO, L. 2011. Caco-2 cells as a model for intestinal absorption. *Curr Protoc Toxicol,* Chapter 20**,** Unit20 6.

ANTONENKO, Y. N., AVETISYAN, A. V., BAKEEVA, L. E., CHERNYAK, B. V., CHERTKOV, V. A., DOMNINA, L. V., IVANOVA, O. Y., IZYUMOV, D. S., KHAILOVA, L. S., KLISHIN, S. S., KORSHUNOVA, G. A., LYAMZAEV, K. G., MUNTYAN, M. S., NEPRYAKHINA, O. K., PASHKOVSKAYA, A. A., PLETJUSHKINA, O. Y., PUSTOVIDKO, A. V., ROGINSKY, V. A., ROKITSKAYA, T. I., RUUGE, E. K., SAPRUNOVA, V. B., SEVERINA, II, SIMONYAN, R. A., SKULACHEV, I. V., SKULACHEV, M. V., SUMBATYAN, N. V., SVIRYAEVA, I. V., TASHLITSKY, V. N., VASSILIEV, J. M., VYSSOKIKH, M. Y., YAGUZHINSKY, L. S., ZAMYATNIN, A. A., JR. & SKULACHEV, V. P. 2008. Mitochondria-targeted plastoquinone derivatives as tools to interrupt execution of the aging program. 1. Cationic plastoquinone derivatives: synthesis and in vitro studies. *Biochemistry (Mosc),* 73**,** 1273-87.

ARAFA EL, S. A., ZHU, Q., SHAH, Z. I., WANI, G., BARAKAT, B. M., RACOMA, I., EL-MAHDY, M. A. & WANI, A. A. 2011. Thymoquinone up-regulates PTEN expression and induces apoptosis in doxorubicin-resistant human breast cancer cells. *Mutat Res,* 706**,** 28-35.

ASADUZZAMAN KHAN, M., TANIA, M., FU, S. & FU, J. 2017. Thymoquinone, as an anticancer molecule: from basic research to clinical investigation. *Oncotarget,* 8**,** 51907-51919.

ASHOUR, A. E., ABD-ALLAH, A. R., KORASHY, H. M., ATTIA, S. M., ALZAHRANI, A. Z., SAQUIB, Q., BAKHEET, S. A., ABDEL-HAMIED, H. E., JAMAL, S. & RISHI, A. K. 2014. Thymoquinone suppression of the human hepatocellular carcinoma cell growth involves inhibition of IL-8 expression, elevated levels of TRAIL receptors, oxidative stress and apoptosis. *Mol Cell Biochem,* 389**,** 85-98.

ASHRAF, W., IBRAHIM, A., ALHOSIN, M., ZAAYTER, L., OUARARHNI, K., PAPIN, C., AHMAD, T., HAMICHE, A., MELY, Y., BRONNER, C. & MOUSLI, M. 2017. The

epigenetic integrator UHRF1: on the road to become a universal biomarker for cancer. *Oncotarget,* 8**,** 51946-51962.

ASLAN, M., AFSAR, E., KIRIMLIOGLU, E., CEKER, T. & YILMAZ, C. 2021. Antiproliferative Effects of Thymoquinone in MCF-7 Breast and HepG2 Liver Cancer Cells: Possible Role of Ceramide and ER Stress. *Nutr Cancer,* 73**,** 460-472.

BAHREINI, F., RAYZAN, E. & REZAEI, N. 2022. MicroRNAs and Diabetes Mellitus Type 1. *Curr Diabetes Rev,* 18**,** e021421191398.

BALLOUT, F., HABLI, Z., RAHAL, O. N., FATFAT, M. & GALI-MUHTASIB, H. 2018. Thymoquinone-based nanotechnology for cancer therapy: promises and challenges. *Drug Discov Today,* 23**,** 1089-1098.

BAYLIN, S. B. & OHM, J. E. 2006. Epigenetic gene silencing in cancer - a mechanism for early oncogenic pathway addiction? *Nat Rev Cancer,* 6**,** 107-16.

BHASKARAN, M. & MOHAN, M. 2014. MicroRNAs: history, biogenesis, and their evolving role in animal development and disease. *Vet Pathol,* 51**,** 759-74.

BHATTACHARJEE, M., UPADHYAY, P., SARKER, S., BASU, A., DAS, S., GHOSH, A., GHOSH, S. & ADHIKARY, A. 2020. Combinatorial therapy of Thymoquinone and Emodin synergistically enhances apoptosis, attenuates cell migration and reduces stemness efficiently in breast cancer. *Biochim Biophys Acta Gen Subj,* 1864**,** 129695.

BILLER, L. H. & SCHRAG, D. 2021. Diagnosis and Treatment of Metastatic Colorectal Cancer: A Review. *JAMA,* 325**,** 669-685.

BRAY, F., LAVERSANNE, M., WEIDERPASS, E. & SOERJOMATARAM, I. 2021. The ever-increasing importance of cancer as a leading cause of premature death worldwide. *Cancer,* 127**,** 3029-3030.

BUSHATI, N. & COHEN, S. M. 2007. microRNA functions. *Annu Rev Cell Dev Biol,* 23**,** 175-205.

CASEY, G. 2016. Genetics, epigenetics and disease. *Nurs N Z,* 22**,** 20-24.

CHEN, C., WANG, Z., DING, Y., WANG, L., WANG, S., WANG, H. & QIN, Y. 2022. DNA Methylation: From Cancer Biology to Clinical Perspectives. *Front Biosci (Landmark Ed),* 27**,** 326.

CHEN, M. C., LEE, N. H., HSU, H. H., HO, T. J., TU, C. C., CHEN, R. J., LIN, Y. M., VISWANADHA, V. P., KUO, W. W. & HUANG, C. Y. 2017. Inhibition of NF-kappaB and metastasis in irinotecan (CPT-11)-resistant LoVo colon cancer cells by thymoquinone via JNK and p38. *Environ Toxicol,* 32**,** 669-678.

CHOMCZYNSKI, P. & SACCHI, N. 2006. The single-step method of RNA isolation by acid guanidinium thiocyanate-phenol-chloroform extraction: twenty-something years on. *Nat Protoc,* 1**,** 581-5.

COLLIGNON, E., CANALE, A., AL WARDI, C., BIZET, M., CALONNE, E., DEDEURWAERDER, S., GARAUD, S., NAVEAUX, C., BARHAM, W., WILSON, A., BOUCHAT, S., HUBERT, P., VAN LINT, C., YULL, F., SOTIRIOU, C., WILLARD-GALLO, K., NOEL, A. & FUKS, F. 2018. Immunity drives TET1 regulation in cancer through NF-kappaB. *Sci Adv,* 4**,** eaap7309.

CORTES-RIOS, J., ZARATE, A. M., FIGUEROA, J. D., MEDINA, J., FUENTES-LEMUS, E., RODRIGUEZ-FERNANDEZ, M., ALIAGA, M. & LOPEZ-ALARCON, C. 2020. Protein quantification by bicinchoninic acid (BCA) assay follows complex kinetics and can be performed at short incubation times. *Anal Biochem,* 608**,** 113904.

COULDREY, C. & CAVE, V. 2014. Assessing DNA methylation levels in animals: choosing the right tool for the job. *Anim Genet,* 45 Suppl 1**,** 15-24.

CRUK. 2021. *Cancer Mortality by Age* [Online]. Available: https://www.cancerresearchuk.org/health-professional/cancer-statistics/mortality/age#heading-Zero [Accessed March 19 2025].

CRUK. 2023. *Side Effects of Cancer Drugs* [Online]. Available: https://www.cancerresearchuk.org/about-cancer/treatment/cancer-drugs/side-effects [Accessed March 19 2025].

DALLI, M., BEKKOUCH, O., AZIZI, S. E., AZGHAR, A., GSEYRA, N. & KIM, B. 2021. Nigella sativa L. Phytochemistry and Pharmacological Activities: A Review (2019-2021). *Biomolecules,* 12.

DERA, A. & RAJAGOPALAN, P. 2019. Thymoquinone attenuates phosphorylation of AKT to inhibit kidney cancer cell proliferation. *J Food Biochem,* 43**,** e12793.

DETICH, N., THEBERGE, J. & SZYF, M. 2002. Promoter-specific activation and demethylation by MBD2/demethylase. *J Biol Chem,* 277**,** 35791-4.

DIORI KARIDIO, I. & SANLIER, S. H. 2021. Reviewing cancer's biology: an eclectic approach. *J Egypt Natl Canc Inst,* 33**,** 32.

DU, Q., LUU, P. L., STIRZAKER, C. & CLARK, S. J. 2015. Methyl-CpG-binding domain proteins: readers of the epigenome. *Epigenomics,* 7**,** 1051-73.

EFTEKHAR, S. P., KAZEMI, S. & MOGHADAMNIA, A. A. 2022. Effect of thymoquinone on pharmacokinetics of 5-fluorouracil in rats and its effect on human cell line in vitro. *Hum Exp Toxicol,* 41**,** 9603271221145422.

EL-ASHRAM, S., AL NASR, I. & SUO, X. 2016. Nucleic acid protocols: Extraction and optimization. *Biotechnol Rep (Amst),* 12**,** 33-39.

EL-SHEHAWY, A. A., ELMETWALLI, A., EL-FAR, A. H., MOSALLAM, S. A. E., SALAMA, A. F., BABALGHITH, A. O., MAHMOUD, M. A., MOHANY, H., GABER, M. & EL-SEWEDY, T. 2023. Thymoquinone, piperine, and sorafenib combinations attenuate liver and breast cancers progression: epigenetic and molecular docking approaches. *BMC Complement Med Ther,* 23**,** 69.

ERFANI, M., ZAMANI, M., TAMADDON, G., HOSSEINI, S. V. & MOKARRAM, P. 2022. Expression and methylation status of BTG2, PPP1CA, and PEG3 genes in colon adenocarcinoma cell lines: promising treatment targets. *Gastroenterol Hepatol Bed Bench,* 15**,** 395-405.

FABBRI, M., GARZON, R., CIMMINO, A., LIU, Z., ZANESI, N., CALLEGARI, E., LIU, S., ALDER, H., COSTINEAN, S., FERNANDEZ-CYMERING, C., VOLINIA, S., GULER, G., MORRISON, C. D., CHAN, K. K., MARCUCCI, G., CALIN, G. A., HUEBNER, K. & CROCE, C. M. 2007. MicroRNA-29 family reverts aberrant methylation in lung cancer by targeting DNA methyltransferases 3A and 3B. *Proc Natl Acad Sci U S A,* 104**,** 15805-10.

FANG, C. Y., WU, C. C., FANG, C. L., CHEN, W. Y. & CHEN, C. L. 2017. Long-term growth comparison studies of FBS and FBS alternatives in six head and neck cell lines. *PLoS One,* 12**,** e0178960.

FANG, J. Y., LU, J., CHEN, Y. X. & YANG, L. 2003. Effects of DNA methylation on expression of tumor suppressor genes and proto-oncogene in human colon cancer cell lines. *World J Gastroenterol,* 9**,** 1976-80.

FOREMAN, K. J., MARQUEZ, N., DOLGERT, A., FUKUTAKI, K., FULLMAN, N., MCGAUGHEY, M., PLETCHER, M. A., SMITH, A. E., TANG, K., YUAN, C. W., BROWN, J. C., FRIEDMAN, J., HE, J., HEUTON, K. R., HOLMBERG, M., PATEL, D. J., REIDY, P., CARTER, A., CERCY, K., CHAPIN, A., DOUWES-SCHULTZ, D., FRANK, T., GOETTSCH, F., LIU, P. Y., NANDAKUMAR, V., REITSMA, M. B., REUTER, V., SADAT, N., SORENSEN, R. J. D., SRINIVASAN, V., UPDIKE, R. L., YORK, H., LOPEZ, A. D., LOZANO, R., LIM, S. S., MOKDAD, A. H., VOLLSET, S. E. & MURRAY, C. J. L. 2018. Forecasting life expectancy, years of life lost, and all-cause and cause-specific mortality for 250 causes of death: reference and alternative scenarios for 2016-40 for 195 countries and territories. *Lancet,* 392**,** 2052-2090.

GARCIA-LOPEZ, J., BRIENO-ENRIQUEZ, M. A. & DEL MAZO, J. 2013. MicroRNA biogenesis and variability. *Biomol Concepts,* 4**,** 367-80.

GARIBYAN, L. & AVASHIA, N. 2013. Polymerase chain reaction. *J Invest Dermatol,* 133**,** 1-4.

GARZON, R., LIU, S., FABBRI, M., LIU, Z., HEAPHY, C. E., CALLEGARI, E., SCHWIND, S., PANG, J., YU, J., MUTHUSAMY, N., HAVELANGE, V., VOLINIA, S., BLUM, W., RUSH, L. J., PERROTTI, D., ANDREEFF, M., BLOOMFIELD, C. D., BYRD, J. C., CHAN, K., WU, L. C., CROCE, C. M. & MARCUCCI, G. 2009. MicroRNA-29b induces global DNA hypomethylation and tumor suppressor gene reexpression in acute myeloid leukemia by targeting directly DNMT3A and 3B and indirectly DNMT1. *Blood,* 113**,** 6411-8.

GHASEMI, M., TURNBULL, T., SEBASTIAN, S. & KEMPSON, I. 2021. The MTT Assay: Utility, Limitations, Pitfalls, and Interpretation in Bulk and Single-Cell Analysis. *Int J Mol Sci,* 22.

GHAZI, T., NAGIAH, S. & CHUTURGOON, A. A. 2022. Fusaric acid induces hepatic global m6A RNA methylation and differential expression of m6A regulatory genes in vivo - a pilot study. *Epigenetics,* 17**,** 695-703.

GLOBAL BURDEN OF DISEASE CANCER, C., KOCARNIK, J. M., COMPTON, K., DEAN, F. E., FU, W., GAW, B. L., HARVEY, J. D., HENRIKSON, H. J., LU, D., PENNINI, A., XU, R., ABABNEH, E., ABBASI-KANGEVARI, M., ABBASTABAR, H., ABD-ELSALAM, S. M., ABDOLI, A., ABEDI, A., ABIDI, H., ABOLHASSANI, H., ADEDEJI, I. A., ADNANI, Q. E. S., ADVANI, S. M., AFZAL, M. S., AGHAALI, M., AHINKORAH, B. O., AHMAD, S., AHMAD, T., AHMADI, A., AHMADI, S., AHMED RASHID, T., AHMED SALIH, Y., AKALU, G. T., AKLILU, A., AKRAM, T., AKUNNA, C. J., AL HAMAD, H., ALAHDAB, F., AL-ALY, Z., ALI, S., ALIMOHAMADI, Y., ALIPOUR, V., ALJUNID, S. M., ALKHAYYAT, M., ALMASI-HASHIANI, A., ALMASRI, N. A., AL-MAWERI, S. A. A., ALMUSTANYIR, S., ALONSO, N., ALVIS-GUZMAN, N., AMU, H., ANBESU, E. W., ANCUCEANU, R., ANSARI, F., ANSARI-MOGHADDAM, A., ANTWI, M. H., ANVARI, D., ANYASODOR, A. E., AQEEL, M., ARABLOO, J., ARAB-ZOZANI, M., AREMU, O., ARIFFIN, H., ARIPOV, T., ARSHAD, M., ARTAMAN, A., ARULAPPAN, J., ASEMI, Z., ASGHARI JAFARABADI, M., ASHRAF, T., ATORKEY, P., AUJAYEB, A., AUSLOOS, M., AWEDEW, A. F., AYALA QUINTANILLA, B. P., AYENEW, T., AZAB, M. A., AZADNAJAFABAD, S., AZARI JAFARI, A., AZARIAN, G., AZZAM,

A. Y., BADIYE, A. D., BAHADORY, S., BAIG, A. A., BAKER, J. L., BALAKRISHNAN, S., BANACH, M., BARNIGHAUSEN, T. W., BARONE-ADESI, F., BARRA, F., BARROW, A., BEHZADIFAR, M., BELGAUMI, U. I., BEZABHE, W. M. M., BEZABIH, Y. M., BHAGAT, D. S., BHAGAVATHULA, A. S., BHARDWAJ, N., BHARDWAJ, P., BHASKAR, S., BHATTACHARYYA, K., et al. 2022. Cancer Incidence, Mortality, Years of Life Lost, Years Lived With Disability, and Disability-Adjusted Life Years for 29 Cancer Groups From 2010 to 2019: A Systematic Analysis for the Global Burden of Disease Study 2019. *JAMA Oncol,* 8**,** 420-444.

GOYAL, S. N., PRAJAPATI, C. P., GORE, P. R., PATIL, C. R., MAHAJAN, U. B., SHARMA, C., TALLA, S. P. & OJHA, S. K. 2017. Therapeutic Potential and Pharmaceutical Development of Thymoquinone: A Multitargeted Molecule of Natural Origin. *Front Pharmacol,* 8**,** 656.

GRAINGER, C. 2023. World Cancer Day 2023: Important Things You Need to Know. *DNA Weekly.*

GUJAR, H., WEISENBERGER, D. J. & LIANG, G. 2019. The Roles of Human DNA Methyltransferases and Their Isoforms in Shaping the Epigenome. *Genes (Basel),* 10.

HANNAN, M. A., RAHMAN, M. A., SOHAG, A. A. M., UDDIN, M. J., DASH, R., SIKDER, M. H., RAHMAN, M. S., TIMALSINA, B., MUNNI, Y. A., SARKER, P. P., ALAM, M., MOHIBBULLAH, M., HAQUE, M. N., JAHAN, I., HOSSAIN, M. T., AFRIN, T., RAHMAN, M. M., TAHJIB-UL-ARIF, M., MITRA, S., OKTAVIANI, D. F., KHAN, M. K., CHOI, H. J., MOON, I. S. & KIM, B. 2021. Black Cumin (Nigella sativa L.): A Comprehensive Review on Phytochemistry, Health Benefits, Molecular Pharmacology, and Safety. *Nutrients,* 13.

HEENEMAN, S., DEUTZ, N. E. & BUURMAN, W. A. 1993. The concentrations of glutamine and ammonia in commercially available cell culture media. *J Immunol Methods,* 166**,** 85-91.

HELMY, S. A., EL-MESERY, M., EL-KAREF, A., EISSA, L. A. & EL GAYAR, A. M. 2019. Thymoquinone upregulates TRAIL/TRAILR2 expression and attenuates hepatocellular carcinoma in vivo model. *Life Sci,* 233**,** 116673.

HNASKO, T. S. & HNASKO, R. M. 2015. The Western Blot. *Methods Mol Biol,* 1318**,** 87-96.

HOLLIDAY, R. 2006. Epigenetics: a historical overview. *Epigenetics,* 1**,** 76-80.

HOMAYOONFAL, M., ASEMI, Z. & YOUSEFI, B. 2021. Targeting microRNAs with thymoquinone: a new approach for cancer therapy. *Cell Mol Biol Lett,* 26**,** 43.

HUSSEIN, S. A., ABDEL-AAL, AMIN, A. & KHALAF, H. A. 2016. Caspase-3, Bcl-2, p53, CYP1A1 and COX -2 as a potential target in chemoprevention of Benzo (a) pyrene-induced lung carcinogenesis in mice: Role of thymoquinone. *International Journal of Chemical and Natural Science***,** 430-441.

IBRAHIM, A., ALHOSIN, M., PAPIN, C., OUARARHNI, K., OMRAN, Z., ZAMZAMI, M. A., AL-MALKI, A. L., CHOUDHRY, H., MELY, Y., HAMICHE, A., MOUSLI, M. & BRONNER, C. 2018. Thymoquinone challenges UHRF1 to commit auto-ubiquitination: a key event for apoptosis induction in cancer cells. *Oncotarget,* 9**,** 28599-28611.

JIANG, H., ZHANG, G., WU, J. H. & JIANG, C. P. 2014. Diverse roles of miR-29 in cancer (review). *Oncol Rep,* 31**,** 1509-16.

KABIL, N., BAYRAKTAR, R., KAHRAMAN, N., MOKHLIS, H. A., CALIN, G. A., LOPEZ-BERESTEIN, G. & OZPOLAT, B. 2018. Thymoquinone inhibits cell proliferation, migration, and invasion by regulating the elongation factor 2 kinase (eEF-2K) signaling axis in triple-negative breast cancer. *Breast Cancer Res Treat,* 171**,** 593-605.

KAPLANEK, R., KEJIK, Z., HAJDUCH, J., VESELA, K., KUCNIROVA, K., SKALICKOVA, M., VENHAUEROVA, A., HOSNEDLOVA, B., HROMADKA, R., DYTRYCH, P., NOVOTNY, P., ABRAMENKO, N., ANTONYOVA, V., HOSKOVEC, D., BABULA, P., MASARIK, M., MARTASEK, P. & JAKUBEK, M. 2023. TET protein inhibitors: Potential and limitations. *Biomed Pharmacother,* 166**,** 115324.

KENSARA, O. A., EL-SHEMI, A. G., MOHAMED, A. M., REFAAT, B., IDRIS, S. & AHMAD, J. 2016. Thymoquinone subdues tumor growth and potentiates the chemopreventive effect of 5-fluorouracil on the early stages of colorectal carcinogenesis in rats. *Drug Des Devel Ther,* 10**,** 2239-53.

KHALIFE, R., HODROJ, M. H., FAKHOURY, R. & RIZK, S. 2016. Thymoquinone from Nigella sativa Seeds Promotes the Antitumor Activity of Noncytotoxic Doses of Topotecan in Human Colorectal Cancer Cells in Vitro. *Planta Med,* 82**,** 312-21.

KHAN, M. A., TANIA, M. & FU, J. 2019. Epigenetic role of thymoquinone: impact on cellular mechanism and cancer therapeutics. *Drug Discov Today,* 24**,** 2315-2322.

KIM, C. & KIM, B. 2018. Anti-Cancer Natural Products and Their Bioactive Compounds Inducing ER Stress-Mediated Apoptosis: A Review. *Nutrients,* 10.

KOHLI, R. M. & ZHANG, Y. 2013. TET enzymes, TDG and the dynamics of DNA demethylation. *Nature,* 502**,** 472-9.

KONG, X., CHEN, J., XIE, W., BROWN, S. M., CAI, Y., WU, K., FAN, D., NIE, Y., YEGNASUBRAMANIAN, S., TIEDEMANN, R. L., TAO, Y., CHIU YEN, R. W., TOPPER, M. J., ZAHNOW, C. A., EASWARAN, H., ROTHBART, S. B., XIA, L. & BAYLIN, S. B. 2019. Defining UHRF1 Domains that Support Maintenance of Human Colon Cancer DNA Methylation and Oncogenic Properties. *Cancer Cell,* 35**,** 633-648 e7.

KOOTI, W., HASANZADEH-NOOHI, Z., SHARAFI-AHVAZI, N., ASADI-SAMANI, M. & ASHTARY-LARKY, D. 2016. Phytochemistry, pharmacology, and therapeutic uses of black seed (Nigella sativa). *Chin J Nat Med,* 14**,** 732-745.

KUBCZAK, M., SZUSTKA, A. & ROGALINSKA, M. 2021. Molecular Targets of Natural Compounds with Anti-Cancer Properties. *Int J Mol Sci,* 22.

KUROWSKA, N., MADEJ, M. & STRZALKA-MROZIK, B. 2023. Thymoquinone: A Promising Therapeutic Agent for the Treatment of Colorectal Cancer. *Curr Issues Mol Biol,* 46**,** 121-139.

KUS, G., OZKURT, M., KABADERE, S., ERKASAP, N., GOGER, G. & DEMIRCI, F. 2018. Antiproliferative and antiapoptotic effect of thymoquinone on cancer cells in vitro. *Bratisl Lek Listy,* 119**,** 312-316.

KWON, J. J., FACTORA, T. D., DEY, S. & KOTA, J. 2019. A Systematic Review of miR-29 in Cancer. *Mol Ther Oncolytics,* 12**,** 173-194.

LIANG, J., ZUBOVITZ, J., PETROCELLI, T., KOTCHETKOV, R., CONNOR, M. K., HAN, K., LEE, J. H., CIARALLO, S., CATZAVELOS, C., BENISTON, R., FRANSSEN, E. & SLINGERLAND, J. M. 2002. PKB/Akt phosphorylates p27, impairs nuclear import of p27 and opposes p27-mediated G1 arrest. *Nat Med,* 8**,** 1153-60.

LIAO, C. H., LAI, I. C., KUO, H. C., CHUANG, S. E., LEE, H. L., WHANG-PENG, J., YAO, C. J. & LAI, G. M. 2019. Epigenetic Modification and Differentiation Induction of Malignant Glioma Cells by Oligo-Fucoidan. *Mar Drugs,* 17.

LIN, R. K. & WANG, Y. C. 2014. Dysregulated transcriptional and post-translational control of DNA methyltransferases in cancer. *Cell Biosci,* 4**,** 46.

LIU, D., DU, Q., ZHU, Y., GUO, Y. & GUO, Y. 2024. UHRF1 knockdown induces cell cycle arrest and apoptosis in breast cancer cells through the ZBTB16/ANXA7/Cyclin B1 axis. *Acta Biochim Biophys Sin (Shanghai),* 56**,** 1633-43.

LIVAK, K. J. & SCHMITTGEN, T. D. 2001. Analysis of relative gene expression data using real-time quantitative PCR and the 2(-Delta Delta C(T)) Method. *Methods,* 25**,** 402-8.

LOPEZ-SERRA, L., BALLESTAR, E., ROPERO, S., SETIEN, F., BILLARD, L. M., FRAGA, M. F., LOPEZ-NIEVA, P., ALAMINOS, M., GUERRERO, D., DANTE, R. & ESTELLER, M. 2008. Unmasking of epigenetically silenced candidate tumor suppressor genes by removal of methyl-CpG-binding domain proteins. *Oncogene,* 27**,** 3556-66.

LU, T. X. & ROTHENBERG, M. E. 2018. MicroRNA. *J Allergy Clin Immunol,* 141**,** 1202-1207.

LUKE, J. J., OTT, P. A. & SHAPIRO, G. I. 2014. The biology and clinical development of MEK inhibitors for cancer. *Drugs,* 74**,** 2111-28.

MAHMOOD, T. & YANG, P. C. 2012. Western blot: technique, theory, and trouble shooting. *N Am J Med Sci,* 4**,** 429-34.

MALIK, S., SINGH, A., NEGI, P. & KAPOOR, V. K. 2021. Thymoquinone: A small molecule from nature with high therapeutic potential. *Drug Discov Today,* 26**,** 2716-2725.

MARTIN, V., JORGENSEN, H. F., CHAUBERT, A. S., BERGER, J., BARR, H., SHAW, P., BIRD, A. & CHAUBERT, P. 2008. MBD2-mediated transcriptional repression of the p14ARF tumor suppressor gene in human colon cancer cells. *Pathobiology,* 75**,** 281-7.

MARTINEZ-LIARTE, J. H., SOLANO, F. & LOZANO, J. A. 1995. Effect of penicillin-streptomycin and other antibiotics on melanogenic parameters in cultured B16/F10 melanoma cells. *Pigment Cell Res,* 8**,** 83-8.

MATSUYAMA, H. & SUZUKI, H. I. 2019. Systems and Synthetic microRNA Biology: From Biogenesis to Disease Pathogenesis. *Int J Mol Sci,* 21.

MAZZOCCOLI, L., ROBAINA, M. C., APA, A. G., BONAMINO, M., PINTO, L. W., QUEIROGA, E., BACCHI, C. E. & KLUMB, C. E. 2018. MiR-29 silencing modulates the expression of target genes related to proliferation, apoptosis and methylation in Burkitt lymphoma cells. *J Cancer Res Clin Oncol,* 144**,** 483-497.

MOORE, L. D., LE, T. & FAN, G. 2013. DNA methylation and its basic function. *Neuropsychopharmacology,* 38**,** 23-38.

MOULANA, M. S., HAIATY, S., BAZMANI, A., SHABKHIZAN, R., MOSLEHIAN, M. S., SADEGHSOLTANI, F., MOSTAFAZADEH, M., ASADI, M. R., TALEBI, M., JAFARI, Z., MOROVATI, M. R., FARZAEI, M. H. & RAHBARGHAZI, R. 2024. Tumoricidal properties of thymoquinone on human colorectal adenocarcinoma cells via the modulation of autophagy. *BMC Complement Med Ther,* 24**,** 132.

NCI. 2022. *Targeted Therapy to Treat Cancer* [Online]. Available: https://www.cancer.gov/about-cancer/treatment/types/targeted-therapies#what-are-the-side-effects-of-targeted-therapy [Accessed March 19 2025].

NCI. 2023. *Immunotherapy Side Effects* [Online]. Available: https://www.cancer.gov/about-cancer/treatment/types/immunotherapy/side-effects [Accessed March 19 2025].

NCI. 2024. *Cancer Statistics* [Online]. Available: https://www.cancer.gov/about-cancer/understanding/statistics [Accessed March 19 2025].

NHS. 2025. *Chemotherapy* [Online]. Available: https://www.nhs.uk/conditions/chemotherapy/ [Accessed March 19 2025].

NISHIYAMA, A. & NAKANISHI, M. 2021. Navigating the DNA methylation landscape of cancer. *Trends Genet,* 37**,** 1012-1027.

OGAWARA, Y., KISHISHITA, S., OBATA, T., ISAZAWA, Y., SUZUKI, T., TANAKA, K., MASUYAMA, N. & GOTOH, Y. 2002. Akt enhances Mdm2-mediated ubiquitination and degradation of p53. *J Biol Chem,* 277**,** 21843-50.

PANG, J., SHEN, N., YAN, F., ZHAO, N., DOU, L., WU, L. C., SEILER, C. L., YU, L., YANG, K., BACHANOVA, V., WEAVER, E., TRETYAKOVA, N. Y. & LIU, S. 2017. Thymoquinone exerts potent growth-suppressive activity on leukemia through DNA hypermethylation reversal in leukemia cells. *Oncotarget,* 8**,** 34453-34467.

PARK, J. W. & HAN, J. W. 2019. Targeting epigenetics for cancer therapy. *Arch Pharm Res,* 42**,** 159-170.

PHESSE, T. J., PARRY, L., REED, K. R., EWAN, K. B., DALE, T. C., SANSOM, O. J. & CLARKE, A. R. 2008. Deficiency of Mbd2 attenuates Wnt signaling. *Mol Cell Biol,* 28**,** 6094-103.

PHUA, C. Y. H., TEOH, Z. L., GOH, B. H., YAP, W. H. & TANG, Y. Q. 2021. Triangulating the pharmacological properties of thymoquinone in regulating reactive oxygen species, inflammation, and cancer: Therapeutic applications and mechanistic pathways. *Life Sci,* 287**,** 120120.

PRABST, K., ENGELHARDT, H., RINGGELER, S. & HUBNER, H. 2017. Basic Colorimetric Proliferation Assays: MTT, WST, and Resazurin. *Methods Mol Biol,* 1601**,** 1-17.

QADI, S. A., HASSAN, M. A., SHEIKH, R. A., BAOTHMAN, O. A., ZAMZAMI, M. A., CHOUDHRY, H., AL-MALKI, A. L., ALBUKHARI, A. & ALHOSIN, M. 2019. Thymoquinone-Induced Reactivation of Tumor Suppressor Genes in Cancer Cells Involves Epigenetic Mechanisms. *Epigenet Insights,* 12**,** 2516865719839011.

QUINLAN, S., KENNY, A., MEDINA, M., ENGEL, T. & JIMENEZ-MATEOS, E. M. 2017. MicroRNAs in Neurodegenerative Diseases. *Int Rev Cell Mol Biol,* 334**,** 309-343.

RAJENDRAN, G., SHANMUGANANDAM, K., BENDRE, A., MUZUMDAR, D., GOEL, A. & SHIRAS, A. 2011. Epigenetic regulation of DNA methyltransferases: DNMT1 and DNMT3B in gliomas. *J Neurooncol,* 104**,** 483-94.

RAMZY, L., METWALLY, A. A., NASR, M. & AWAD, G. A. S. 2020. Novel thymoquinone lipidic core nanocapsules with anisamide-polymethacrylate shell for colon cancer cells overexpressing sigma receptors. *Sci Rep,* 10**,** 10987.

RASMUSSEN, K. D. & HELIN, K. 2016. Role of TET enzymes in DNA methylation, development, and cancer. *Genes Dev,* 30**,** 733-50.

RAWLA, P., SUNKARA, T. & BARSOUK, A. 2019. Epidemiology of colorectal cancer: incidence, mortality, survival, and risk factors. *Prz Gastroenterol,* 14**,** 89-103.

RAZIN, A. & KANTOR, B. 2005. DNA methylation in epigenetic control of gene expression. *Prog Mol Subcell Biol,* 38**,** 151-67.

ROY, P. S. & SAIKIA, B. J. 2016. Cancer and cure: A critical analysis. *Indian J Cancer,* 53**,** 441-442.

RYAN, B. J. & HENEHAN, G. T. 2017. Avoiding Proteolysis During Protein Purification. *Methods Mol Biol,* 1485**,** 53-69.

SAKAMOTO, S., PUTALUN, W., VIMOLMANGKANG, S., PHOOLCHAROEN, W., SHOYAMA, Y., TANAKA, H. & MORIMOTO, S. 2018. Enzyme-linked immunosorbent assay for the quantitative/qualitative analysis of plant secondary metabolites. *J Nat Med,* 72**,** 32-42.

SAMARGHANDIAN, S., AZIMI-NEZHAD, M. & FARKHONDEH, T. 2019. Thymoquinone-induced antitumor and apoptosis in human lung adenocarcinoma cells. *J Cell Physiol,* 234**,** 10421-10431.

SARKAR, C., JAMADDAR, S., ISLAM, T., MONDAL, M., ISLAM, M. T. & MUBARAK, M. S. 2021. Therapeutic perspectives of the black cumin component thymoquinone: A review. *Food Funct,* 12**,** 6167-6213.

SCHNEIDER-STOCK, R., FAKHOURY, I. H., ZAKI, A. M., EL-BABA, C. O. & GALI-MUHTASIB, H. U. 2014. Thymoquinone: fifty years of success in the battle against cancer models. *Drug Discov Today,* 19**,** 18-30.

SHAHIN, Y. R., ELGUINDY, N. M., ABDEL BARY, A. & BALBAA, M. 2018. The protective mechanism of Nigella sativa against diethylnitrosamine-induced hepatocellular carcinoma through its antioxidant effect and EGFR/ERK1/2 signaling. *Environ Toxicol*.

SIDHU, H. & CAPALASH, N. 2017. UHRF1: The key regulator of epigenetics and molecular target for cancer therapeutics. *Tumour Biol,* 39**,** 1010428317692205.

SOLEIMANI, A., RAHMANI, F., SAEEDI, N., GHAFFARIAN, R., KHAZAEI, M., FERNS, G. A., AVAN, A. & HASSANIAN, S. M. 2019. The potential role of regulatory microRNAs of RAS/MAPK signaling pathway in the pathogenesis of colorectal cancer. *J Cell Biochem,* 120**,** 19245-19253.

STIRZAKER, C., SONG, J. Z., NG, W., DU, Q., ARMSTRONG, N. J., LOCKE, W. J., STATHAM, A. L., FRENCH, H., PIDSLEY, R., VALDES-MORA, F., ZOTENKO, E. & CLARK, S. J. 2017. Methyl-CpG-binding protein MBD2 plays a key role in maintenance and spread of DNA methylation at CpG islands and shores in cancer. *Oncogene,* 36**,** 1328-1338.

SUBRAMANIAM, D., THOMBRE, R., DHAR, A. & ANANT, S. 2014. DNA methyltransferases: a novel target for prevention and therapy. *Front Oncol,* 4**,** 80.

SUTTON, K. M., GREENSHIELDS, A. L. & HOSKIN, D. W. 2014. Thymoquinone, a bioactive component of black caraway seeds, causes G1 phase cell cycle arrest and apoptosis in triple-negative breast cancer cells with mutant p53. *Nutr Cancer,* 66**,** 408-18.

UDDIN, M. S., MAMUN, A. A., ALGHAMDI, B. S., TEWARI, D., JEANDET, P., SARWAR, M. S. & ASHRAF, G. M. 2022. Epigenetics of glioblastoma multiforme: From molecular mechanisms to therapeutic approaches. *Semin Cancer Biol,* 83**,** 100-120.

VAGHARI-TABARI, M., FERNS, G. A., QUJEQ, D., ANDEVARI, A. N., SABAHI, Z. & MOEIN, S. 2021. Signaling, metabolism, and cancer: An important relationship for therapeutic intervention. *J Cell Physiol,* 236**,** 5512-5532.

VELLINGIRI, B., IYER, M., DEVI SUBRAMANIAM, M., JAYARAMAYYA, K., SIAMA, Z., GIRIDHARAN, B., NARAYANASAMY, A., ABDAL DAYEM, A. & CHO, S. G. 2020. Understanding the Role of the Transcription Factor Sp1 in Ovarian Cancer: from Theory to Practice. *Int J Mol Sci,* 21.

WADDINGTON, C. H. 2012. The epigenotype. 1942. *Int J Epidemiol,* 41**,** 10-3.

WANG, L., YANG, X., ZHAO, K., HUANG, S., QIN, Y., CHEN, Z., HU, X., JIN, G. & ZHOU, Z. 2024a. MOF-mediated acetylation of UHRF1 enhances UHRF1 E3 ligase activity to facilitate DNA methylation maintenance. *Cell Rep,* 43**,** 113908.

WANG, S., WANG, M., ICHINO, L., BOONE, B. A., ZHONG, Z., PAPAREDDY, R. K., LIN, E. K., YUN, J., FENG, S. & JACOBSEN, S. E. 2024b. MBD2 couples DNA

methylation to transposable element silencing during male gametogenesis. *Nat Plants,* 10**,** 13-24.

WANG, Y., WANG, C., ZHONG, R., WANG, L. & SUN, L. 2024c. Research progress of DNA methylation in colorectal cancer (Review). *Mol Med Rep,* 30.

WHO 2023. Colorectal Cancer. *WHO.*

WOOD, K. H. & ZHOU, Z. 2016. Emerging Molecular and Biological Functions of MBD2, a Reader of DNA Methylation. *Front Genet,* 7**,** 93.

WRONSKA, A. 2023. The Role of microRNA in the Development, Diagnosis, and Treatment of Cardiovascular Disease: Recent Developments. *J Pharmacol Exp Ther,* 384**,** 123-132.

WU, Q. & NI, X. 2015. ROS-mediated DNA methylation pattern alterations in carcinogenesis. *Curr Drug Targets,* 16**,** 13-9.

WU, X. & ZHANG, Y. 2017. TET-mediated active DNA demethylation: mechanism, function and beyond. *Nat Rev Genet,* 18**,** 517-534.

XIE, Y., LIU, B., PAN, J., LIU, J., LI, X., LI, H., QIU, S., XIANG, X., ZHENG, P., CHEN, J., YUAN, Y., DONG, Z. & ZHANG, D. 2021. MBD2 Mediates Septic AKI through Activation of PKCeta/p38MAPK and the ERK1/2 Axis. *Mol Ther Nucleic Acids,* 23**,** 76-88.

YANG, J., KUANG, X. R., LV, P. T. & YAN, X. X. 2015. Thymoquinone inhibits proliferation and invasion of human nonsmall-cell lung cancer cells via ERK pathway. *Tumour Biol,* 36**,** 259-69.

ZHANG, J., PAVLOVA, N. N. & THOMPSON, C. B. 2017. Cancer cell metabolism: the essential role of the nonessential amino acid, glutamine. *EMBO J,* 36**,** 1302-1315.

ZHANG, L., BAI, Y. & YANG, Y. 2016. Thymoquinone chemosensitizes colon cancer cells through inhibition of NF-kappaB. *Oncol Lett,* 12**,** 2840-2845.

ZHANG, L., LU, Q. & CHANG, C. 2020a. Epigenetics in Health and Disease. *Adv Exp Med Biol,* 1253**,** 3-55.

ZHANG, M., DU, H., HUANG, Z., ZHANG, P., YUE, Y., WANG, W., LIU, W., ZENG, J., MA, J., CHEN, G., WANG, X. & FAN, J. 2018a. Thymoquinone induces apoptosis in bladder cancer cell via endoplasmic reticulum stress-dependent mitochondrial pathway. *Chem Biol Interact,* 292**,** 65-75.

ZHANG, M., DU, H., WANG, L., YUE, Y., ZHANG, P., HUANG, Z., LV, W., MA, J., SHAO, Q., MA, M., LIANG, X., YANG, T., WANG, W., ZENG, J., CHEN, G., WANG, X. & FAN, J. 2020b. Thymoquinone suppresses invasion and metastasis in bladder cancer

cells by reversing EMT through the Wnt/beta-catenin signaling pathway. *Chem Biol Interact,* 320**,** 109022.

ZHANG, Y., FAN, Y., HUANG, S., WANG, G., HAN, R., LEI, F., LUO, A., JING, X., ZHAO, L., GU, S. & ZHAO, X. 2018b. Thymoquinone inhibits the metastasis of renal cell cancer cells by inducing autophagy via AMPK/mTOR signaling pathway. *Cancer Sci,* 109**,** 3865-3873.

ZHU, C., CAI, Y., MO, S., ZHU, J., WANG, W., PENG, B., GUO, J., ZHANG, Z. & CHEN, X. 2021. NF-kappaB-mediated TET2-dependent TNF promoter demethylation drives Mtb-upregulation TNF expression in macrophages. *Tuberculosis (Edinb),* 129**,** 102108.

ZHU, D., HUNTER, S. B., VERTINO, P. M. & VAN MEIR, E. G. 2011. Overexpression of MBD2 in glioblastoma maintains epigenetic silencing and inhibits the antiangiogenic function of the tumor suppressor gene BAI1. *Cancer Res,* 71**,** 5859-70.

APPENDIX A

BCA assay

The absorbances of the BSA standards were used to construct a standard curve (Figure 6.1) from which concentrations of the protein samples were determined. The samples were then standardised (Table 6.1).

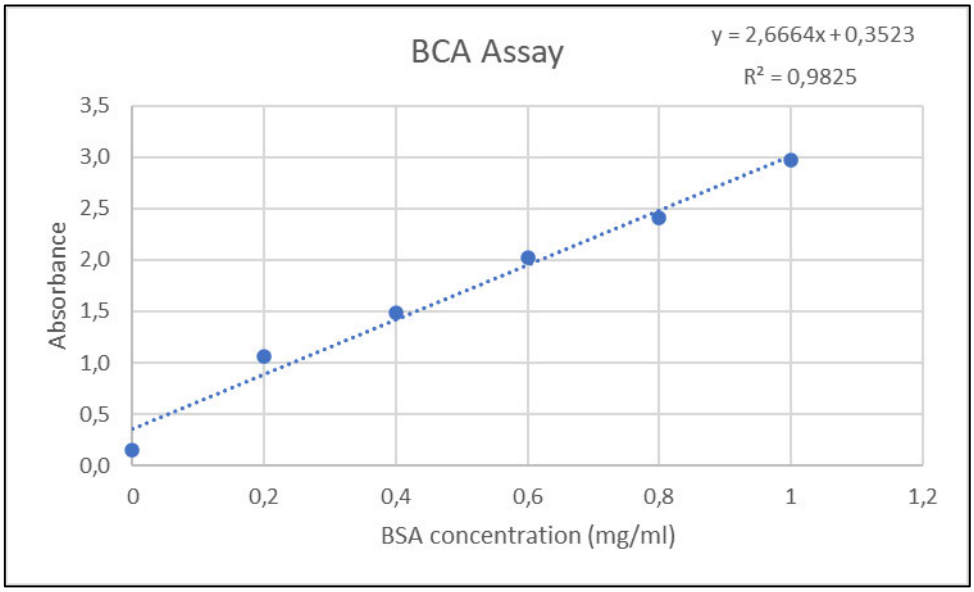

Figure 6.1: BCA standard curve for protein quantification and standardisation.

Table 5: Standardisation of protein samples (Final volume: 200 µL; Final concentration: 0.35 mg/ml).

Sample	**Absorbance**	**Concentration (mg/ml)**	**Volume of protein (µL)**	**Volume of Cytobuster (µL)**
Control	3.498	1.180	59.32	140.68
504 µM TQ	1.608	0.471	148.62	51.38
DMSO	3.253	1.088	64.34	135.66

APPENDIX B

ELISA

An ELISA kit was used for the quantification of DNMT3b. The optical density of the given DNMT3b standards were used to construct a standard curve (Figure 6.2), from which the sample DNMT3b concentrations were extrapolated.

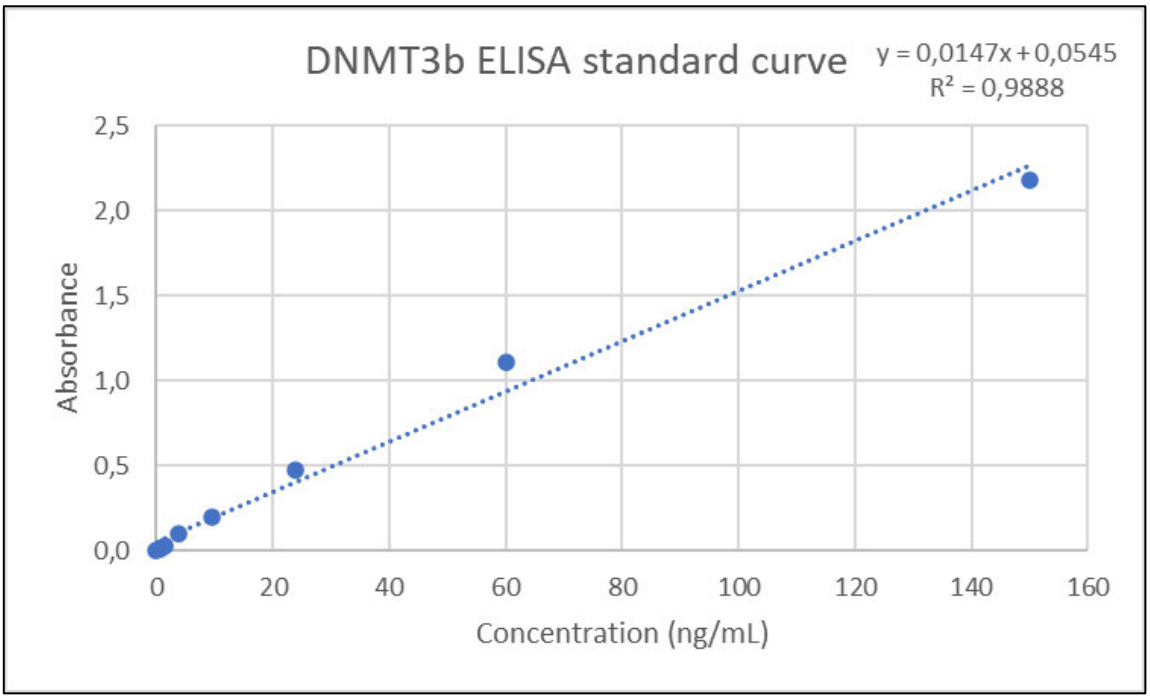

Figure 6.2: Standard curve for DNMT3b ELISA.

APPENDIX C

Quantification of global DNA methylation

A colorimetric kit was used for the quantification of global DNA methylation. The optical densities of the given 5mC standards were used to construct a standard curve (Figure 6.3), from which the percentage of 5mC in the DNA samples were determined.

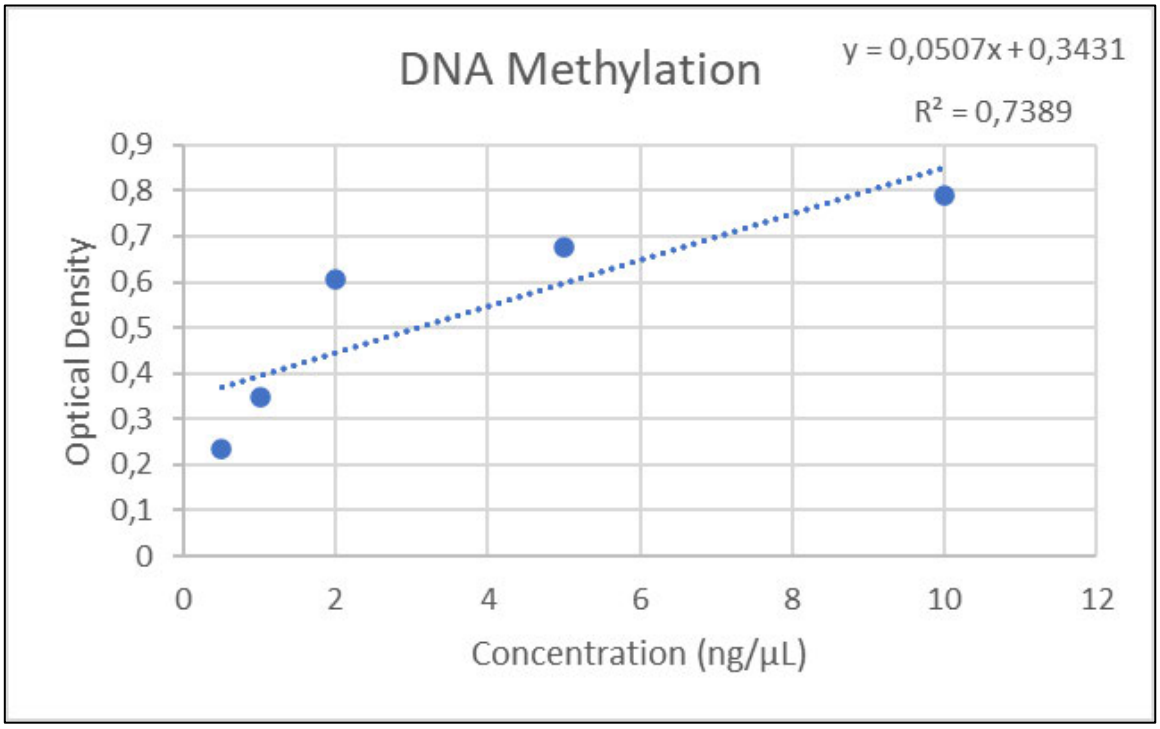

Figure 6.3: Standard curve for quantification of DNA methylation.

APPENDIX D

UNIVERSITY OF KWAZULU-NATAL
INYUVESI YAKWAZULU-NATALI

11 October 2023

Ms Aaliyah Mangerah (222010501)
School of Lab Med & Medical Sc
Howard College

Dear Ms Mangerah,

Protocol reference number: BREC/00006233/2023
Project title: An investigation into the effects of Thymoquinone on DNA methylation status of U-87 MG cells
Degree Purposes: MMedSc

EXPEDITED APPLICATION: APPROVAL LETTER

A sub-committee of the Biomedical Research Ethics Committee has considered and noted your application.

The conditions have been met and the study is given full ethics approval and may begin as from 11 October 2023. Please ensure that any outstanding site permissions are obtained and forwarded to BREC for approval before commencing research at a site.

This approval is valid for one year from 11 October 2023. To ensure uninterrupted approval of this study beyond the approval expiry date, an application for recertification must be submitted to BREC on RIG on the appropriate BREC form 2-3 months before the expiry date.

Any amendments to this study, unless urgently required to ensure safety of participants, must be approved by BREC prior to implementation.

Your acceptance of this approval denotes your compliance with South African National Research Ethics Guidelines (2015), South African National Good Clinical Practice Guidelines (2020) (if applicable) and with UKZN BREC ethics requirements as contained in the UKZN BREC Terms of Reference and Standard Operating Procedures, all available at http://research.ukzn.ac.za/Research-Ethics/Biomedical-Research-Ethics.aspx.

BREC is registered with the South African National Health Research Ethics Council (REC-290408-009). BREC has US Office for Human Research Protections (OHRP) Federal-wide Assurance (FWA 678).

The sub-committee's decision will be noted by a full Committee at its next meeting taking place on 14 November 2023.

Yours sincerely,

[redacted]

Prof D Wassenaar
Chair: Biomedical Research Ethics Committee

Biomedical Research Ethics Committee
Chair: Professor D R Wassenaar
UKZN Research Ethics Office Westville Campus, Govan Mbeki Building
Postal Address: Private Bag X54001, Durban 4000
Email: BREC@ukzn.ac.za
Website: http://research.ukzn.ac.za/Research-Ethics/Biomedical-Research-Ethics.aspx

Founding Campuses: Edgewood Howard College Medical School Pietermaritzburg Westville

INSPIRING GREATNESS

Figure 6.4: BREC approval letter.